AD NUMBER

AD875612

LIMITATION CHANGES

TO:

Approved for public release; distribution is unlimited. Document partially illegible.

FROM:

Distribution authorized to U.S. Gov't. agencies and their contractors; Critical Technology; AUG 1970. Other requests shall be referred to Army Engineer Waterways Experiment Station, Vicksburg, MS 39181. This document contains export-controlled technical data.

AUTHORITY

usaewes ltr, 27 jul 1971

TECHNICAL REPORT NO. 3-783

AN ANALYTICAL MODEL FOR PREDICTING CROSS-COUNTRY VEHICLE PERFORMANCE

APPENDIX F: SOIL-VEHICLE RELATIONS ON SOFT CLAY SOILS (SURFACE COMPOSITION)

by

C. A. Blackmon

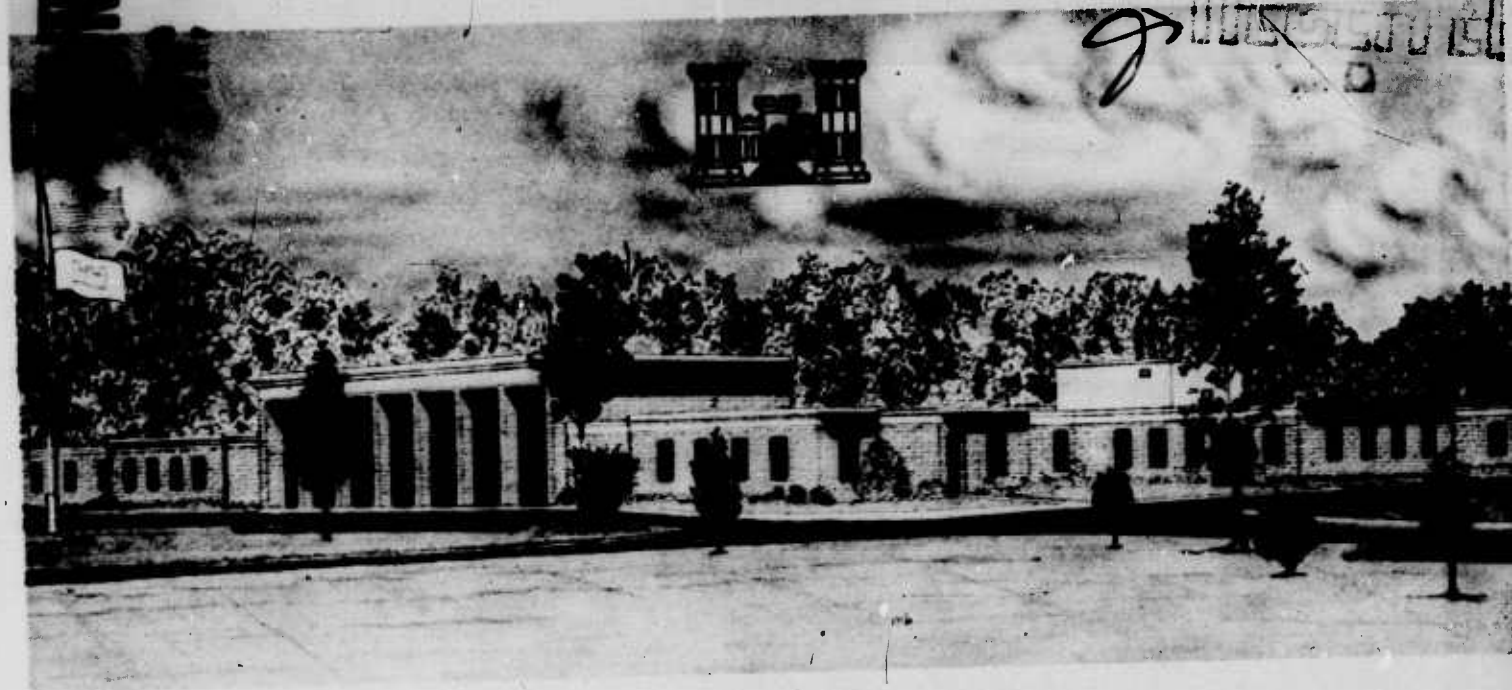

August 1970

Sponsored by Advanced Research Projects Agency

and

Directorate of Development and Engineering, U. S. Army Materiel Command

Service Agency U. S. Army Materiel Command

Conducted by U. S. Army Engineer Waterways Experiment Station, Vicksburg, Mississippi 39181

DISCLAIMER NOTICE

THIS DOCUMENT IS THE BEST QUALITY AVAILABLE.

COPY FURNISHED CONTAINED A SIGNIFICANT NUMBER OF PAGES WHICH DO NOT REPRODUCE LEGIBLY.

MISSING PAGE
NUMBERS ARE BLANK
AND WERE NOT
FILMED

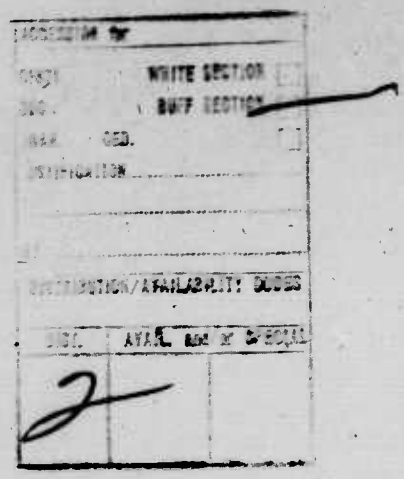

Destroy this report when no longer needed. Do not return it to the originator.

The findings in this report are not to be construed as an official Department of the Army position unless so designated by other authorized documents.

TECHNICAL REPORT NO. 3-783

AN ANALYTICAL MODEL FOR PREDICTING CROSS-COUNTRY VEHICLE PERFORMANCE

APPENDIX F: SOIL-VEHICLE RELATIONS ON SOFT CLAY SOILS (SURFACE COMPOSITION)

by

C. A. Blackmon

August 1970

Sponsored by Advanced Research Projects Agency

Directorate of Development and Engineering, U. S. Army Materiel Command

Service Agency U. S. Army Materiel Command

Project Nos. 1-T-0-62112-A-131 and 1-T-0-62103-A-046-02

Conducted by U. S. Army Engineer Waterways Experiment Station, Vicksburg, Mississippi

ARMY-MRC VICKSBURG, MISS.

THE CONTENTS OF THIS REPORT ARE NOT TO BE USED FOR ADVERTISING, PUBLICATION, OR PROMOTIONAL PURPOSES. CITATION OF TRADE NAMES DOES NOT CONSTITUTE AN OFFICIAL ENDORSEMENT OR APPROVAL OF THE USE OF SUCH COMMERCIAL PRODUCTS.

FOREWORD

The study reported herein was performed by the U. S. Army Engineer Waterways Experiment Station (WES) for the Office, Secretary of Defense (OSD), Advanced Research Projects Agency (ARPA), and is a portion of one task of the overall Mobility Environmental Research Study (MERS) sponsored by OSD/ARPA for which the WES was the prime contractor and the U. S. Army Materiel Command (AMC) was the service agent. The broad mission of Project MERS was to determine the effects of the various features of the physical environment on the performance of cross-country ground contact vehicles and to provide therefrom data that can be used to improve both the design and employment of such vehicles. A condition of the project was that the data be interpretable in terms of vehicle requirements for Southeast Asia. The funds employed for this study were allocated to WES through AMC under ARPA Order No. 400. Some funds for preparation and publication of this report were provided by the Directorate of Development and Engineering, AMC, under Department of the Army Project 1-T-0-62112-A-131, Environmental Constraints on Materiel, and Project 1-T-0-62103-A-046-02 "Surface Mobility." The field work was performed during the period June 1964 to November 1965, under the general guidance and supervision of the MERS Branch of the WES, the staff element of WES responsible for the technical management and direction of the MERS program.

This appendix is one of seven to the report entitled An Analytical Model for Predicting Cross-Country Vehicle Performance. These appendixes are:

A. Instrumentation of Test Vehicles

B. Vehicle Performance in Lateral and Longitudinal Obstacles (Vegetation)

Volume I: Lateral Obstacles

Volume II: Longitudinal Obstacles

C. Vehicle Performance in Vertical Obstacles (Surface Geometry)

D. Performance of Amphibious Vehicles in the Water-Land Interface (Hydrologic Geometry)

E. Quantification of the Screening Effects of Vegetation on Driver's Vision and Vehicle Speed

F. Soil-Vehicle Relations on Soft Clay Soils (Surface Composition)

G. Application of Analytical Model to United States and Thailand Terrains

The study was conducted by personnel of the Mobility and Environmental (M&E) Division, under the general supervision of Mr. W. J. Turnbull, Technical Assistant for Soils and Engineering (retired); Mr. W. G. Shockley and Mr. S. J. Knight, Chief and Assistant Chief, respectively, M&E Division; Mr. A. A. Rula, Chief, Vehicle Studies Branch; Mr. W. E. Grabau, Chief, Terrain Analysis Branch; and Mr. J. K. Stoll, Chief, Obstacle-Vehicle Studies Section. Special acknowledgment is made to Mr. E. S. Rush, Chief, Soil-Vehicle Studies Section, and Mr. N. R. Murphy, Engineer, Vehicle Dynamics Section, who provided guidance for portions of the analysis. The tests reported herein were supervised by Mr. B. G. Stinson. Major assistance in the preparation of plates and tables was provided by Mr. J. L. Lee. This report was written by Mr. C. A. Blackmon.

Directors of WES during this study and the preparation of this report were COL Alex G. Sutton, Jr., CE, COL John R. Oswalt, Jr., CE, COL Levi A. Brown, CE, and COL Ernest D. Peixotto, CE. Technical Directors were Messrs. J. B. Tiffany and F. R. Brown.

CONTENTS

CONVERSION FACTORS, BRITISH TO METRIC UNITS OF MEASUREMENT

British units of measurement used in this report can be converted to metric units as follows:

Multiply	By	To Obtain
inches	2.54	centimeters
feet	0.3048	meters
miles (U. S. statute)	1.609344	kilometers
pounds	0.45359237	kilograms
short tons (2000 lb)	907.185	kilograms
pounds per square inch	0.070307	kilograms per square centimeter
feet per second	0.3048	meters per second
miles per hour	1.609344	kilometers per hour

SUMMARY

Sixty-six acceleration-deceleration tests were conducted with three wheeled and two tracked vehicles at five sites in Thailand. The principal conclusion from these tests was that vehicle deceleration in soft clay soils can be correlated with soil strength expressed as the average 0- to 6-in. cone index. The analysis indicated that acceleration increased with an increase in soil strength, but no definitive correlation could be established. Semiempirical and empirical relations were used in a first-generation analytical model to predict average speed over the test courses. Comparisons of measured and predicted speeds led to recommendations for specific additional studies to improve the reliability of the WES analytical model.

AN ANALYTICAL MODEL FOR PREDICTING CROSS-COUNTRY VEHICLE PERFORMANCE

APPENDIX F: SOIL-VEHICLE RELATIONS ON SOFT CLAY SOILS (SURFACE COMPOSITION)

PART I: INTRODUCTION

Background

1. The main text of this report describes the development of an analytical model for predicting the cross-country performance of a vehicle. The model was based on an energy concept within the framework of classical mechanics that requires cause-and-effect relations be established between discrete terrain factors and vehicle response. The terrain factors considered in the analytical model are (a) surface geometry, (b) surface composition, (c) vegetation, and (d) hydrologic geometry. This appendix deals with limited aspects of the surface composition factor--the effects of soil strength on the acceleration and deceleration of the vehicle.

2. Previous and concurrent studies in the field and laboratory have yielded empirical and semiempirical correlations of soil strength and vehicle performance in terms of minimum strength negotiable, motion resistance, and drawbar pull. A method of predicting vehicle performance while accelerating and decelerating has been presented in a recent report;[1] however, no actual vehicle performance tests were included in that study.

Purpose and Scope

3. This appendix describes acceleration-deceleration tests conducted by the U. S. Army Engineer Waterways Experiment Station (WES) in Thailand during the period 12-30 October 1965. The general purpose of these tests was to obtain data relating characteristics of soft clay soil to vehicle performance in terms suitable for use in developing that portion of the analytical model for predicting cross-country performance. The specific purpose was to determine if vehicle performance in terms of

acceleration and deceleration could be related to soil strength. An additional purpose of this report was to compare the average speeds predicted by the WES analytical model using both empirical and semiempirical correlations of soil strength and vehicle performance with the average speeds measured in field tests.

4. Sixty-six tests were conducted with three wheeled and two tracked vehicles at five sites in Thailand. Surface composition of all sites in terms of the Unified Soil Classification System (USCS) was a fat clay (CH); the average soil strengths in the 0- to 6-in.* layer ranged from 16 to 71 cone index.

* A table of factors for converting British units of measurement to metric units is presented on page ix.

PART II: TEST PROGRAM

Location and Description of Test Areas

5. The tests reported herein were conducted at three general locations in Thailand: Pran Buri, Phet Buri, and Samut Prakan (fig. F1). Descriptions of the test sites at the time the tests were conducted are given in the following paragraphs.

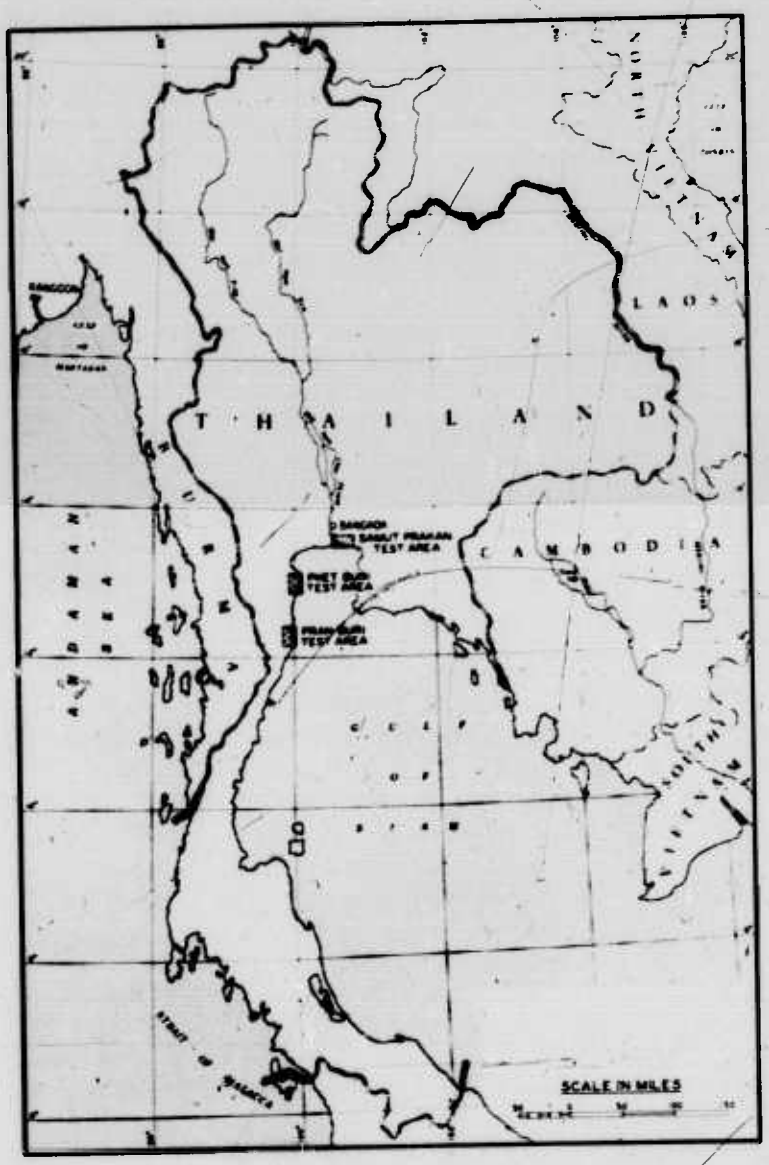

Fig. F1. Vicinity map; Samut Prakan, Phet Buri, and Pran Buri test sites

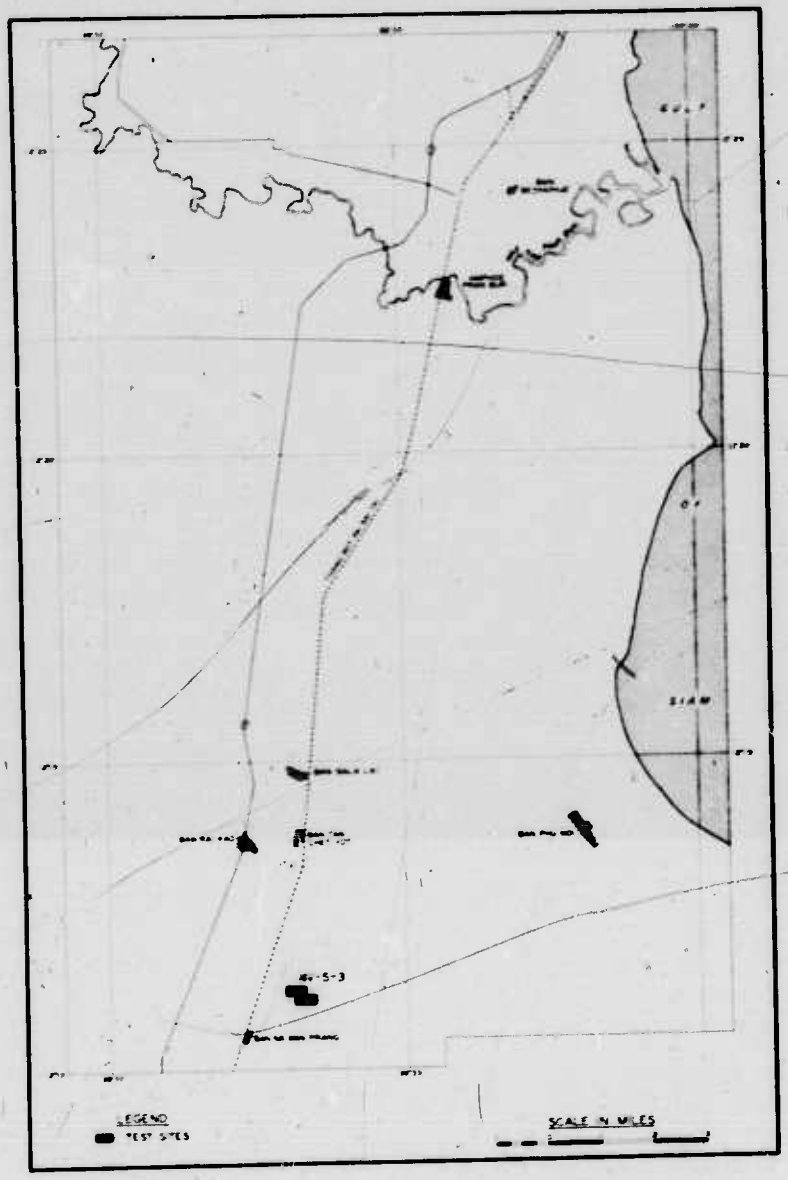

Fig. F2. Location of Pran Buri test site

Pran Buri

6. Test site 4V-S-3 was located about 14 miles south of Pran Buri near the village of Na Wan Priang (fig. F2) in a grass-covered, low-lying area dissected by drainage canals. The site was approximately 300 ft long and 200 ft wide and very nearly level (less than 0.5 percent slope). As stated previously, the soil at the site (and also at the four other test sites) was classified as CH according to the USCS. The average cone index of the 0- to 6-in. layer ranged from 54 to 71. The site was free of surface irregularities (fig. F3a).

a. Grass-covered surface at site 4V-S-3

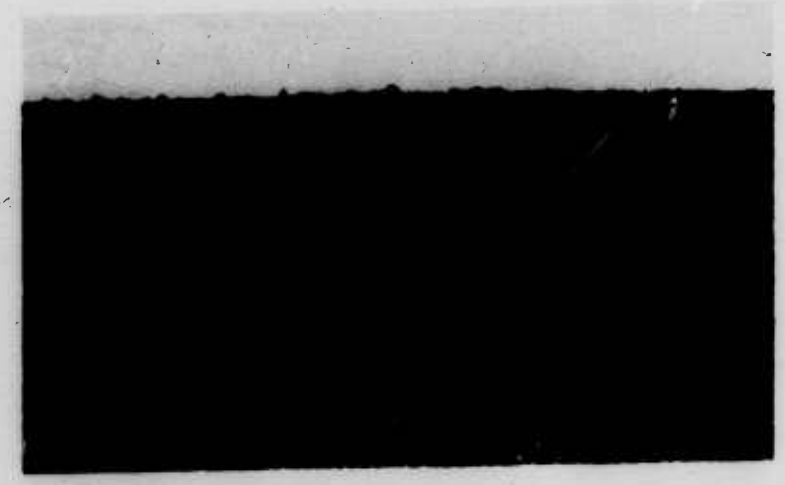

b. 4- to 8-in.-deep surface water at site MRDC-X_6

c. Small-scale surface irregularities at site MRDC-X_4

Fig. F3. Surface conditions at three test sites

Phet Buri

7. Test site MRDC-X_{10} was located about 11 miles southeast of Phet Buri (fig. F4) in a low-lying area containing no vegetation. The site was approximately 300 ft long and 200 ft wide and very nearly level (less than 0.5 percent slope). The average cone index of the 0- to 6-in. layer ranged from 41 to 64. The site was free of surface irregularites.

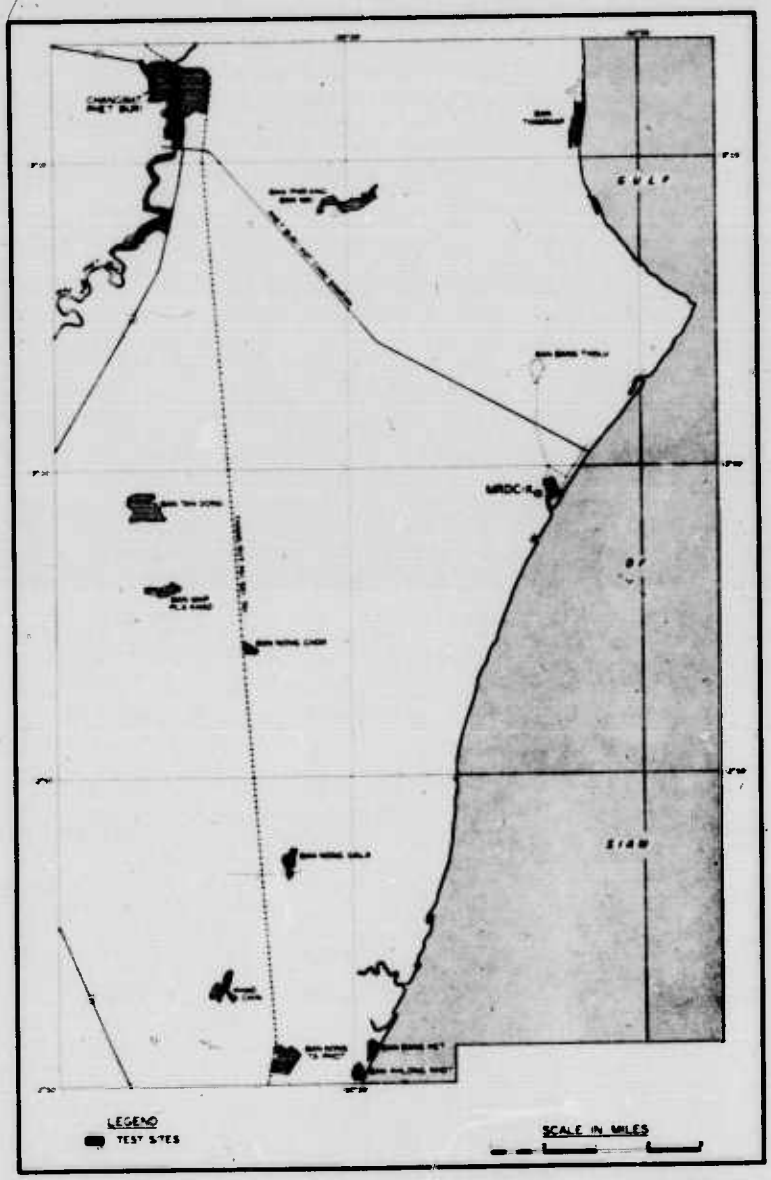

Fig. F4. Location of Phet Buri test site

Samut Prakan

8. Three test sites were located in the Samut Prakan test area (fig. F5). Test site MRDC-X_2 was about 6 miles southeast of Samut Prakan; test sites MRDC-X_4 and MRDC-X_6 were near the village of Tambon Khlong Dan. All were in low-lying areas containing no vegetation. Each was approximately 300 ft long and 100 ft wide. They were oriented so that the slope of each test lane was less than 1.0 percent. At the time of testing, site MRDC-X_2 was covered with 3 to 6 in. of water, site MRDC-X_6 with 4 to 8 in. of water (fig. F3b), and site MRDC-X_4 was very wet but nearly free of surface water. The average cone index of the 0- to 6-in. layer ranged from 29 to 43 at site MRDC-X_2, from 27 to 42 at site MRDC-X_4, and from 16 to 20 at site MRDC-X_6. The small-scale surface irregularities that were present at all the sites in the Samut Prakan area were judged insignificant from the standpoint of vehicle performance (fig. F3c).

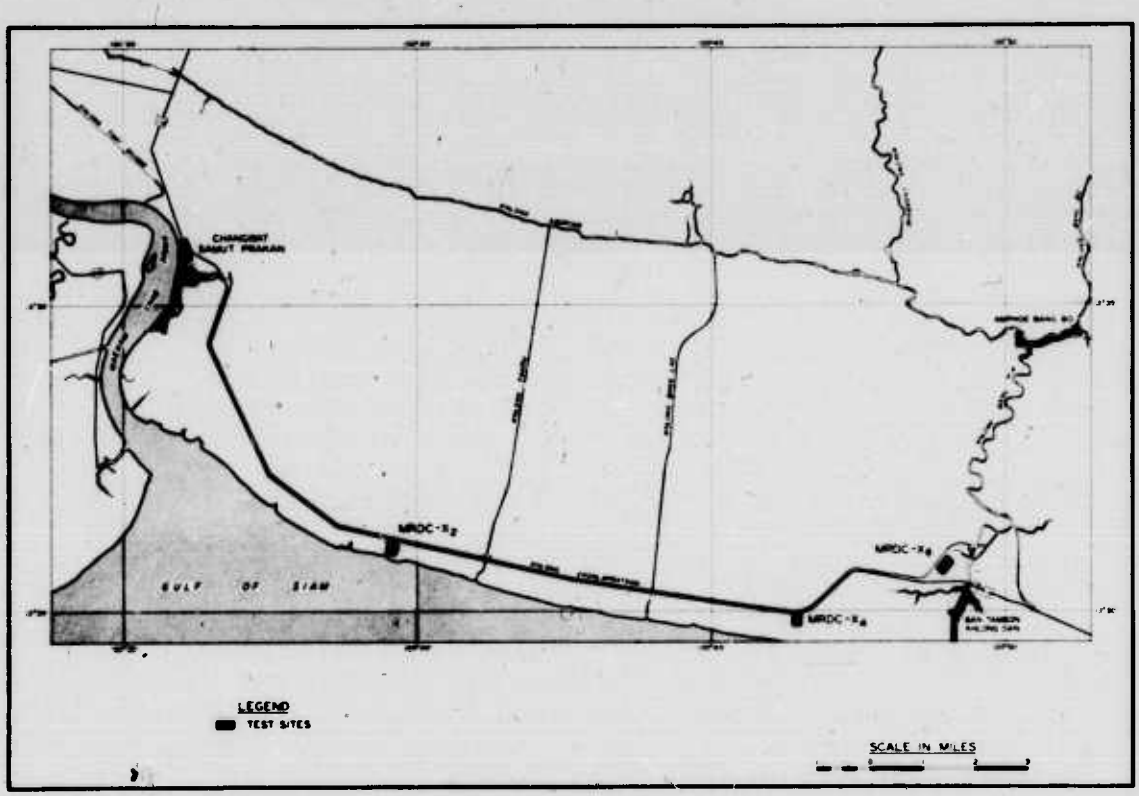

Fig. F5. Location of Samut Prakan test sites

Vehicles Used

9. Three wheeled vehicles--the M151 1/4-ton utility truck, the M37 3/4-ton cargo truck, and the M35A1 2-1/2-ton cargo truck--and two tracked vehicles--the M29C amphibious cargo carrier and the M113 armored personnel carrier--were used in these tests (fig. F6). Pertinent physical

a. M151 1/4-ton utility truck

b. M37 3/4-ton cargo truck

c. M35A1 2-1/2-ton cargo truck

d. M29C amphibious cargo carrier

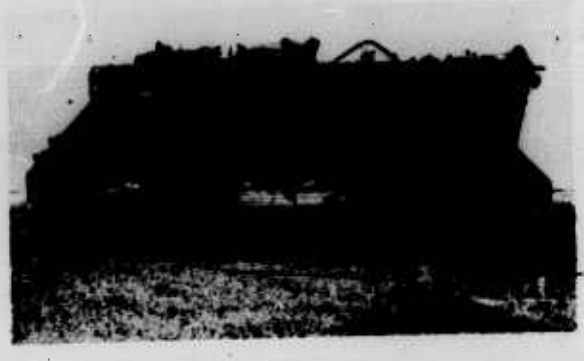

e. M113 armored personnel carrier

Fig. F6. Wheeled and tracked vehicles used in test program

characteristics of the vehicles are given in table F1.

10. All test vehicles were equipped with fairly elaborate measuring and recording systems. This instrumentation is discussed in detail in reference 2.

Tests Conducted

11. The acceleration-deceleration tests conducted in this study were considered as being of two types on the basis of the manner in which the deceleration in each test was accomplished. When the vehicle was brought to a stop by free-rolling, i.e. with the clutch disengaged, the test was considered to be an acceleration-rolling test (identified by the letter R following the test number); when the vehicle was brought to a stop by application of the brakes, the test was considered to be an acceleration-braking test (identified by the letter B following the test number). Tests employing both methods of deceleration were conducted with each vehicle, although not at each site. The following tabulation shows the number and type of tests conducted with each vehicle at each test site.

	Vehicle and Type of Test										Total Tests	
	M151		M37		M35A1		M29C		M113			
Test Site	R	B	R	B	R	B	R	B	R	B	R	B
4V-S-3	2	1	3	2	3	2	2	1	3	2	13	8
MRDC-X_{10}	3	2	3	3	2	2	2	1	2	0	12	8
MRDC-X_2	3	2	3	0	2	0	0	0	0	0	8	2
MRDC-X_4	3	2	2	0	0	0	3	2	0	0	8	4
MRDC-X_6	0	0	0	0	0	0	3	0	0	0	3	0
Total	11	7	11	5	7	4	10	4	5	2	44	22

Test Procedures and Performance Data Obtained

12. The vehicle was positioned at the beginning of the 300-ft-long test lane and the driver was instructed to accelerate the vehicle as quickly as possible to a point that would allow ample room for deceleration without overrunning the test course, and then to disengage the clutch (in

the acceleration-rolling tests) and allow the vehicle to roll to a stop or to apply the brakes (in the acceleration-braking tests) and bring the vehicle to a stop. The wheeled vehicles and the M29C, all having manual transmissions, were usually started in second gear, low range, and shifted to third gear, low range. The M113, the only vehicle with automatic transmission in the test program, was operated in gear range 3-4 in six tests and in gear range 1-2 in one test. Poles were placed at 50-ft intervals along the edge of the test lane to serve as reference points and to assist the driver in following a straight-line course (fig. F7). Since it was

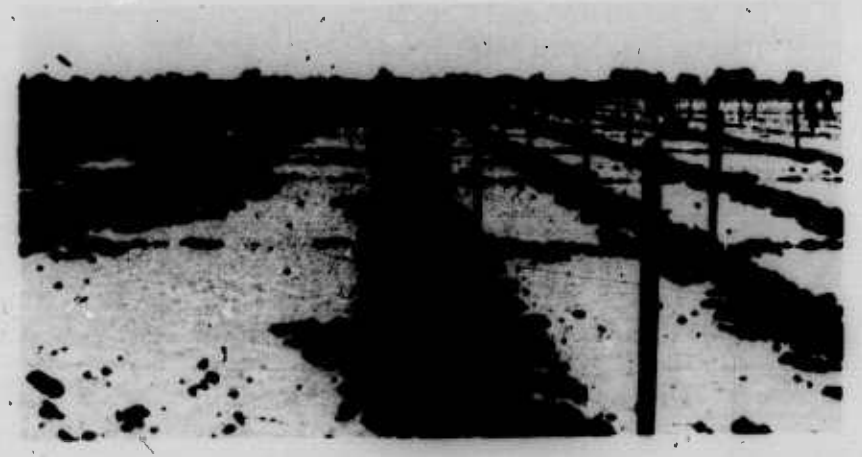

Fig. F7. Site MRDC-X_{10}. Poles at edge of test lane assisted driver in following course and served as reference points

believed that variation in driving ability, for instance in the time required to effect a gear change, might affect the test results, the same driver was used throughout the test program.

13. By means of electronic instrumentation installed on the test vehicles, continuous measurements of time, distance traveled, drive-shaft revolutions, and wheel or track rotational speed were made and recorded on oscillograms. In addition, for some tests drive-line torque and longitudinal acceleration were measured and recorded. A surveyor's chain was used to validate total distance traveled and a stopwatch was used to obtain a check on total time. Appropriate data from the tests are summarized in table F2. Voluminous data were obtained in reducing the oscillograms to a more convenient-to-use form. For example, distance traveled, vehicle

speed, wheel or track speed, percent wheel or track slip, and average acceleration or deceleration of the vehicle were determined and tabulated for each second of each test. In the interests of economy, these data are not reproduced in this appendix but are filed at WES for future reference.

Soil Data Obtained

Soil samples

14. Samples for classification of the soil according to the USCS were obtained from the 0- to 6-in. and 6- to 12-in. soil layers from each test site. A summary of the laboratory data is included in table F3. Grain-size distribution curves are shown in figs. F8 and F9.

Cone index

15. Cone indexes were measured at the surface and at depths of 1, 2, 3, 4, 5, 6, 9, and 12 in. at 6-ft intervals along each side of the test lane prior to testing. In some tests, the vehicle straddled one of the ruts of a preceding test and the previously collected soil data were deemed adequate. Following each test, the portion of the lane in which the vehicle was accelerating and the portion in which the vehicle was decelerating were determined. A summary of the cone index data is given in table F4.

Other Data Obtained

16. Other data obtained included photographs, miscellaneous measurements, notes, and observations. Data not included in this appendix are filed at WES for future reference.

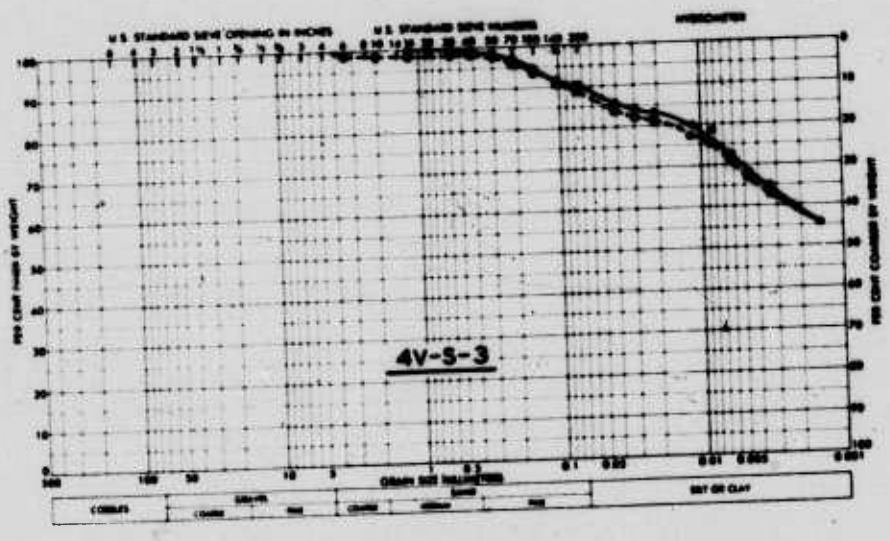

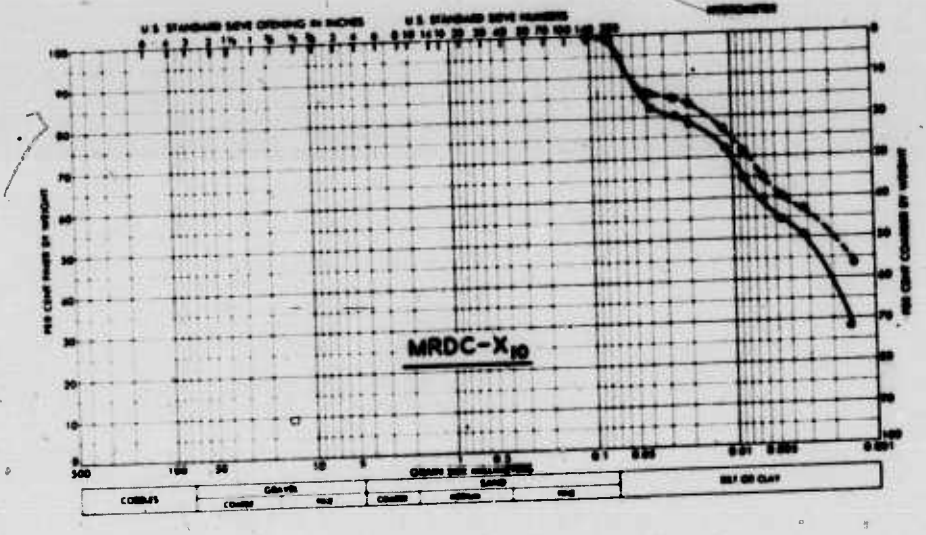

LEGEND

——— 0- TO 6-IN. LAYER

- - - - - - 6- TO 12-IN. LAYER

Fig. F8. Grain-size distribution of soils at Pran Buri (4V-S-3) and Phet Buri (MRDC-X_{10}) test sites

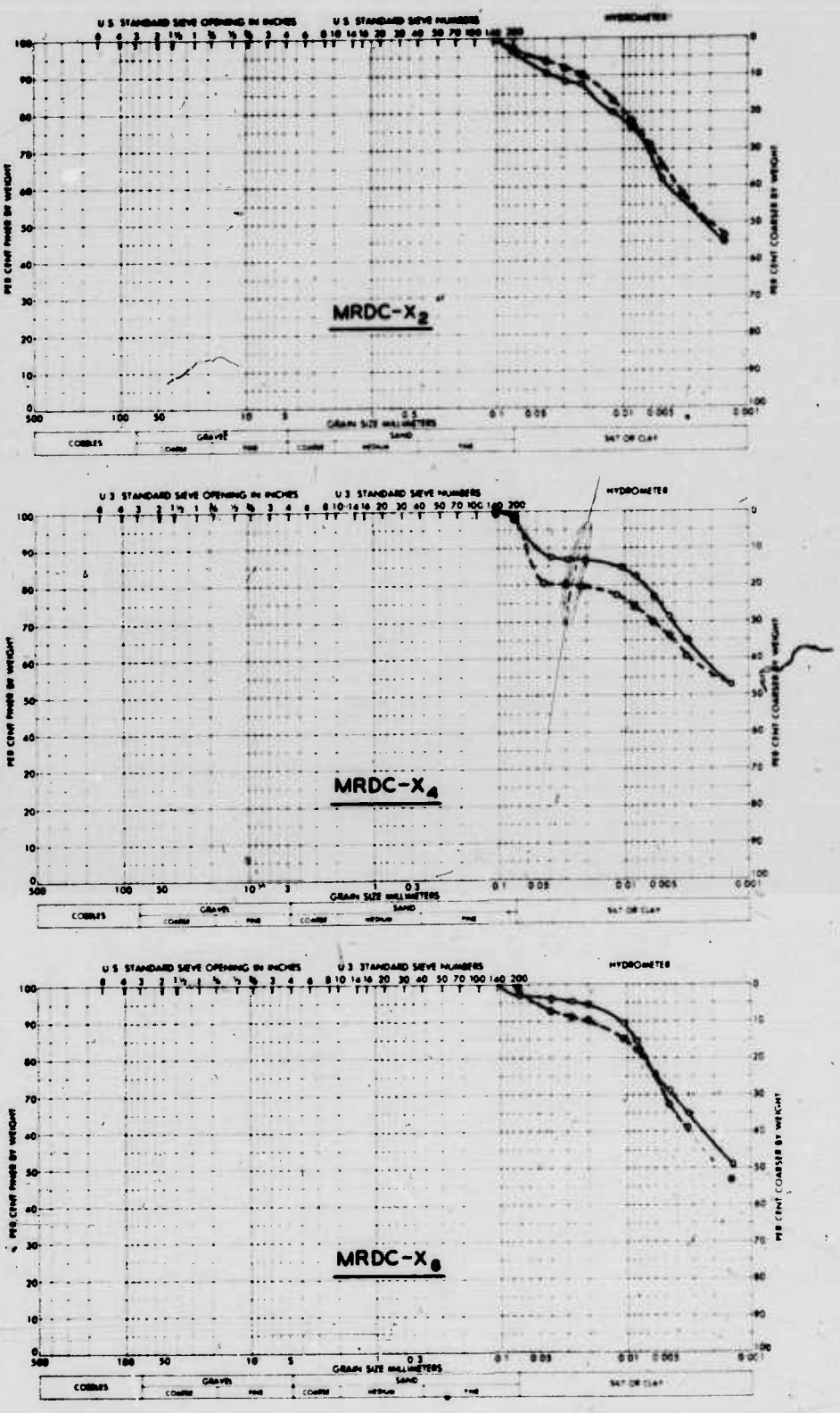

Fig. F9. Grain-size distribution of soils at Samut Prakan test sites

PART III: ANALYSIS OF DATA

17. The data collected in this test program were analyzed to determine if acceleration and deceleration of vehicles could be related to soil strength and to evaluate the accuracy of current prediction techniques for vehicles accelerating and decelerating over short distances.

Basis of Analysis

18. Acceleration is, by definition, the time rate of change of velocity. Mathematically, this may be expressed by the equation

$$\frac{V_2 - V_1}{t} = a \qquad (1)$$

where

V_1, V_2 = speed at the beginning and end, respectively, of an increment of time, fps

t = time increment, sec

a = acceleration, ft/sec^2

When the speed at the end of the increment (V_2) is less than the speed at the beginning of the increment (V_1), the acceleration is negative and is termed deceleration ($-a$). Equation 1 in various forms is used throughout the analysis; other special considerations and equations peculiar to a particular part of the analysis are discussed as they are introduced.

Acceleration Relations

19. The acceleration a given vehicle can achieve depends on that vehicle's characteristics (weight, engine performance, transmission efficiency, etc.), the skill of the driver (in steering, feeding fuel to the engine, shifting gears, etc.), and the condition of the surface on which the vehicle operates. In these tests, changes in the characteristics of a given vehicle that occurred between tests or within a test were not considered to be significant, and driver effects were minimized (but not eliminated) by using the same driver in all tests. Thus, even though the tests lacked consistency (distance or time in which acceleration occurred

was not the same in all tests) and no attempt was made to attain a maximum velocity because of the prohibitive length of the test course that would have been required, it was felt that some quantitative estimate of the effect of soil strength on acceleration could be made. Fig. F10 shows the

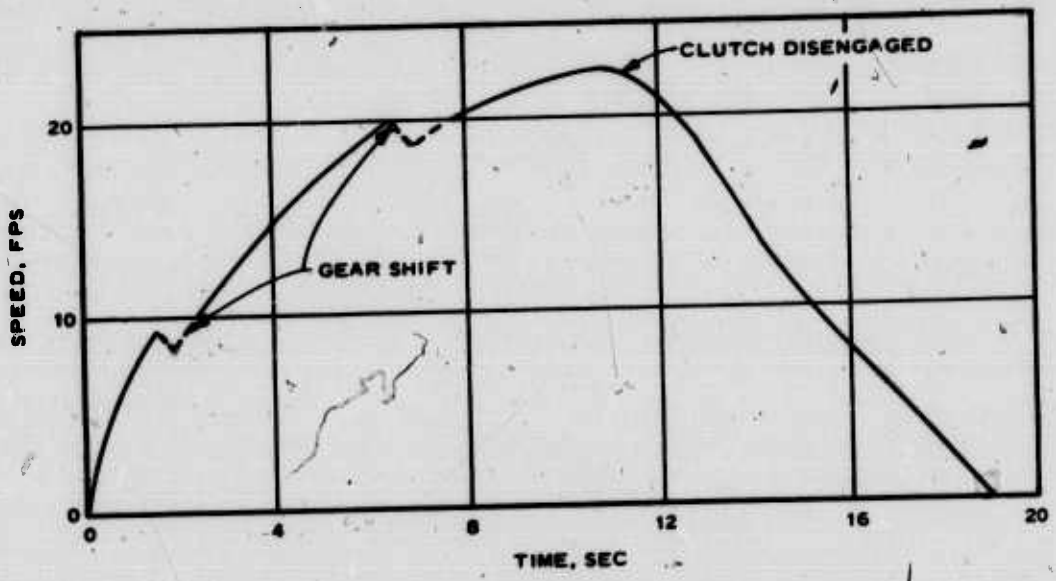

Fig. F10. Speed-time curve for test 269 R. (Data from which this plot was constructed are given in table F10)

speed-time curve for a typical test. It is to be noted that acceleration (slope of the curve) was constantly changing; dashed portions of the curve represent the abrupt change when the gears were shifted. Several plots of acceleration and/or velocity versus soil strength were made as follows:

Parameter	Soil Strength
Maximum acceleration (usually occurred during first 1-sec time increment of test)	Average 0- to 6-in. cone index of the corresponding portion of the test lane
Average acceleration until time clutch was disengaged	Average 0- to 6-in. cone index of the corresponding portion of the test lane
Average acceleration during first 5 sec	Average 0- to 6-in. cone index of the corresponding portion of the test lane
Average velocity for first 100 ft	Average 0- to 6-in. cone index of the corresponding portion of the test lane

20. All these plots showed a fairly general effect of cone index on acceleration. The plots that appeared most informative were those of maximum acceleration versus the average 0- to 6-in. cone index for that portion of the test lane where the maximum acceleration occurred. These plots are discussed in the following paragraphs.

Wheeled vehicles

21. Plots of maximum acceleration versus the average 0- to 6-in. cone index are shown in plate F1. Results from tests conducted on bare surfaces are indicated by open symbols; results from tests on grass-covered surfaces are indicated by closed symbols. While the limited range of strengths in each surface-cover group and the obvious scatter of data for M151 tests (fig. a, plate F1) seem to preclude drawing a definitive curve through the data points, some trends are evident. The increase in acceleration with an increase in soil strength for the M37 and M35A1 tests (figs. b and c, plate F1) is impressive, and it may be noted, especially in fig. b, that the closed symbols appear as a logical extension of the open symbols, suggesting to some extent that the soil strength has a greater influence upon acceleration than does the surface cover.

Tracked vehicles

22. Plots of maximum acceleration versus the average 0- to 6-in. cone index are shown in plate F2 for the two tracked vehicles. Again, while no curves are presented, it may be seen that there is a trend toward an increase in acceleration with an increase in soil strength.

Deceleration Relations

23. The deceleration of a vehicle depends upon that vehicle's characteristics (weight, traction element contact area, internal resistance when rolling, and how quickly the wheels or tracks can be locked when advantageous for braking), the skill of the driver (in steering, application of brakes, etc.), and the condition of the surface on which the vehicle operates. In the rolling tests, changes in the characteristics of a given vehicle between tests were not considered to be significant, and the driver effects were minimized (but not eliminated) by using the same driver in all

tests. In the braking tests changes in the vehicle's characteristics were deemed significant. For example, it was not always possible to lock the brakes, particularly when the brake drums became wet (fig. F11). Additionally, during the braking tests at some of the grass-covered sites, the grass sheared irregularly (fig. F12). It is believed that these factors were, in part, responsible for the highly variable results of the braking tests. Since an investigation of these factors was not within the scope of this program, only the tests in which deceleration was accomplished by disengaging the power train and allowing the vehicle to roll freely to a stop are considered in this part of the analysis.

24. For most of the tests considered, the deceleration for each 1-sec time interval from the time the power train was disengaged until the vehicle stopped rolling was fairly constant (see fig. F10). In a few cases (one M151 test, six M37 tests, and one M113 test) malfunction of the distance play-out line prevented a second-by-second determination for the entire period of deceleration; therefore, the value of deceleration expressed as $-a/g$ given in table F2 was determined over less than the full period of deceleration.

Wheeled vehicles

25. Plots of average deceleration versus the average 0- to 6-in. cone index are shown in plate F3 for the three wheeled vehicles tested. The curves drawn in figs. a, b, and c, plate F3, represent the lines of visual best fit. The minimum soil strength required for one pass (VCI_1) is shown for each vehicle. It was computed by a semiempirical method now being developed at WES.* It may be noted that the deceleration for the M151 is higher than that for the other two vehicles at approximately the same soil strength. This may be explained in part by realizing that deceleration represents the result of all forces resisting motion of the vehicle, including the surface condition, and it would be expected that water or a

---

* Work in progress and curves relating a computed mobility index to the vehicle cone index required for one pass and fifty passes of a vehicle on level soil are described in "Quarterly Progress Report on Waterways Experiment Station Research and Development Projects" for the first quarter of 1969.

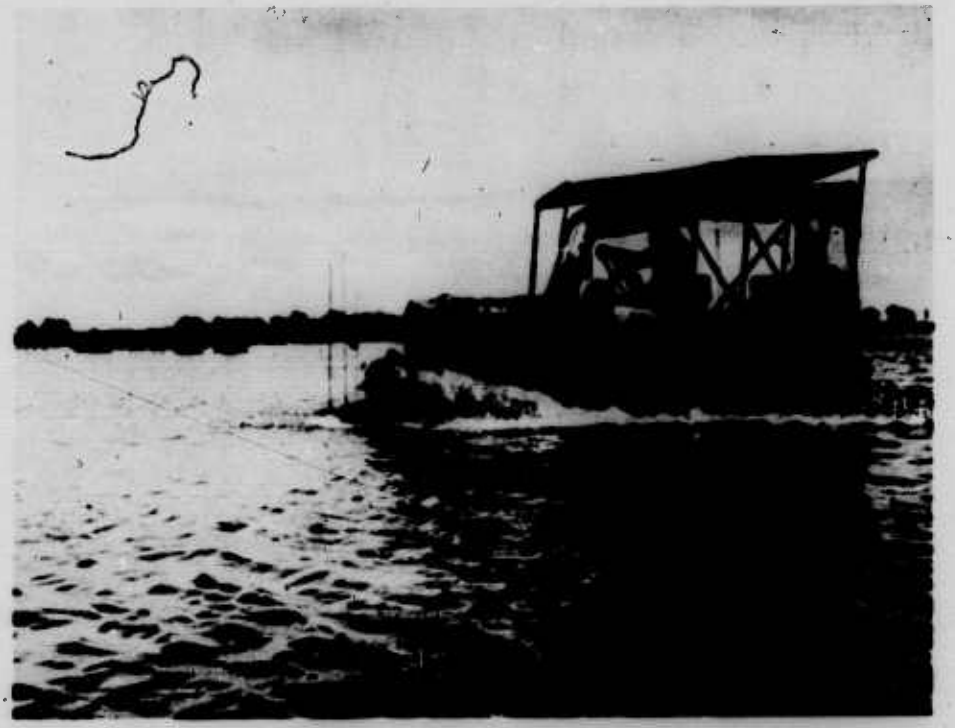

Fig. F11. Splashing water wet the brakes at site MRDC-X_2

Fig. F12. Note grass shear during deceleration by braking at site 4V-S-3

slushy surface condition (such as that encountered in these tests) would have a greater retarding effect, percentagewise, on the smaller and lighter M151 than on the heavier and larger M37 and M35A1. For this reason, in fig. d, plate F3 (where the deceleration values for all three wheeled vehicles were plotted against soil strength expressed as cone index points above VCI_1 to establish a single relation), the location of the curve was influenced to a greater extent by the M37 and M35A1 data points than by the M151 data points. The location and curvature of the line in fig. d are admittedly arbitrary and somewhat provisory. The extrapolation as indicated by the dashed line is based on results of other studies in the field and laboratory that indicate that the towed force-soil strength relation becomes asymptotic at a force/weight ratio of approximately 0.30. Data in this region are extremely scarce, and it is emphasized that the relation expressed by the curve in fig. d, plate F3, may be changed when additional data become available. Nevertheless, the curve in fig. d does define a relation between deceleration and soil strength that appears reasonable.

Tracked vehicles

26. Plots of deceleration versus soil strength expressed as the average 0- to 6-in. cone index are shown in figs. a and b, plate F4, for the M29C and the M113, respectively. The summary plot (fig. c) indicates that the data correlate quite well when soil strength is expressed as cone index points above VCI_1. The curves drawn through the data points represent lines of visual best fit. The extrapolation of the curve on the summary plot follows the same reasoning as that for the summary plot (fig. d, plate F3) given in the preceding paragraph. Examination of the data presented in plate F4 indicates that while the decrease in deceleration with an increase in soil strength is very small, the correlation is good and the curves adequately define the relation of deceleration and soil strength within the limits encountered in this program.

Prediction of Vehicle Performance

27. Although the tests were not typical of normal vehicle operation, they did furnish some data in terms of average speed of real vehicles over

sections (albeit short) of natural terrain that could be used for comparison with average speeds predicted by current modeling techniques, and, in a sense, serve to validate the relations established in this and concurrent test programs. To this end, predictions were made of the average speed and compared with the measured average speed in 52 tests. Of the 66 tests, data for 14 tests were incomplete and are not used in this portion of the analysis. The prediction techniques are described and illustrated by example in the following paragraphs.

Pavement-vehicle relations

28. The WES analytical model for predicting cross-country performance of military vehicles begins with a basic relation peculiar to each vehicle that expresses the maximum tractive force that can be developed at any speed on a firm, level surface (e.g. pavement). The relation for a particular vehicle may be obtained empirically by drawbar pull-speed and motion resistance-speed tests on a firm, level surface or may be computed from engine performance data, taking into account propulsion system losses. The pavement data used in these predictions are shown graphically in plate F5 and in tabular form in table F5. The data sources are indicated in table F5.

Soil-vehicle relations

29. The next step in the WES analytical model is to establish the effects of soil strength by using the maximum drawbar pull and motion resistance values for the vehicle and particular soil condition. Ideally, these values would be determined by actual field tests on the same soil condition for which the speed prediction is being made. Since this is not always practicable, a part of the overall Mobility Environmental Research Study (MERS) program was concerned with developing methods of predicting maximum drawbar pull and motion resistance and with exploring methods previously developed. In this study, for the soil condition in each area, the maximum drawbar pull and the motion resistance for each wheeled vehicle were predicted by two methods--identified herein as the WES numeric and the WES curves. Predictions for the tracked vehicle utilized only the latter method since the WES numeric at this time is applicable only to wheeled vehicles.

30. WES numeric. The development and use of the WES numeric have been described in several reports[1,3,4] and only the equations are repeated here:

$$N = \frac{Cbd}{W} \cdot \left(\frac{\delta}{h}\right)^{1/2} \tag{2}$$

$$\frac{P_t}{W} = \frac{0.4072}{N - 0.8713} - 0.0206 \tag{3}$$

$$\frac{P_{20}}{W} = \frac{N - 2.25}{6.2 + 0.45N} \tag{4}$$

where

N = WES numeric

C = average cone index of 0- to 6-in. soil layer

b = width of tire, in.

d = diameter of tire, in.

W = weight, lb; in using the equations in this report, W was obtained by dividing the gross weight of each vehicle by the number of wheels on which the vehicle was operating

δ = tire deflection, in.

h = section height of tire, in.

P_t = towed force, lb

P_{20} = drawbar pull at 20 percent slip, lb

Equations 2, 3, and 4 refer to a single wheel. Where the computed values of P_{20}/W and P_t/W are used in this report in reference to a specific vehicle, they are considered as being equivalent to drawbar pull coefficient (DBP/W) and motion resistance coefficient (MR/W), respectively. The relations expressed by the WES numeric were developed from tests on laboratory prepared soils of uniform strength and moisture content. More recently, tests have been conducted at WES to determine the effects on performance when the soil is flooded. Results[5] have indicated that a 40 percent decrease in pull may be expected when the surface of a clay soil is wet or flooded. Since the surfaces of the test areas in this study

were predominantly wet or flooded, the P_{20}/W values determined by equation 4 were reduced by 40 percent and are identified as 60 percent drawbar pull coefficient in table F6. The same reference indicated no reason to alter the P_t/W values as computed by equation 3. These are identified as motion resistance coefficients in table F6.

31. WES curves. The alternate set of soil-vehicle relations used to predict maximum drawbar pull and motion resistance is identified as the WES curves. Values of maximum drawbar pull, expressed as DBP/W , were obtained from curves (fig. F13) developed in reference 6. These curves

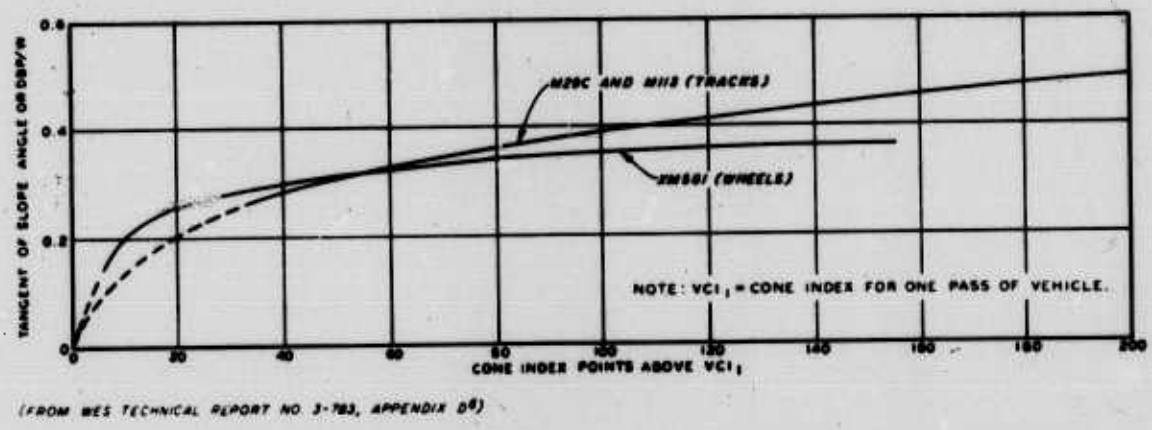

Fig. F13. Performance of tracked and wheeled vehicles in the water-land interface, fine-grained soils

were derived from drawbar pull and slope-climbing tests of wheeled and tracked vehicles on flooded and wet surface soils, which is essentially the same surface condition that existed in the tests reported herein. Values of motion resistance, expressed as MR/W , were obtained from the deceleration relations given in plates F3 and F4. (An explanation of the rationale is given in paragraph 35). Values of both maximum drawbar pull and motion resistance as determined by the WES curves for use in these predictions are given in table F6.

32. Adjustment of pavement performance curve. The DBP/W and MR/W values determined by each method and a tractive force-slip relation were used to adjust the pavement curves for effects of soil strength and wheel or track slip to determine tractive coefficient-speed and drawbar pull coefficient-speed curves on soil. An example of this procedure is given

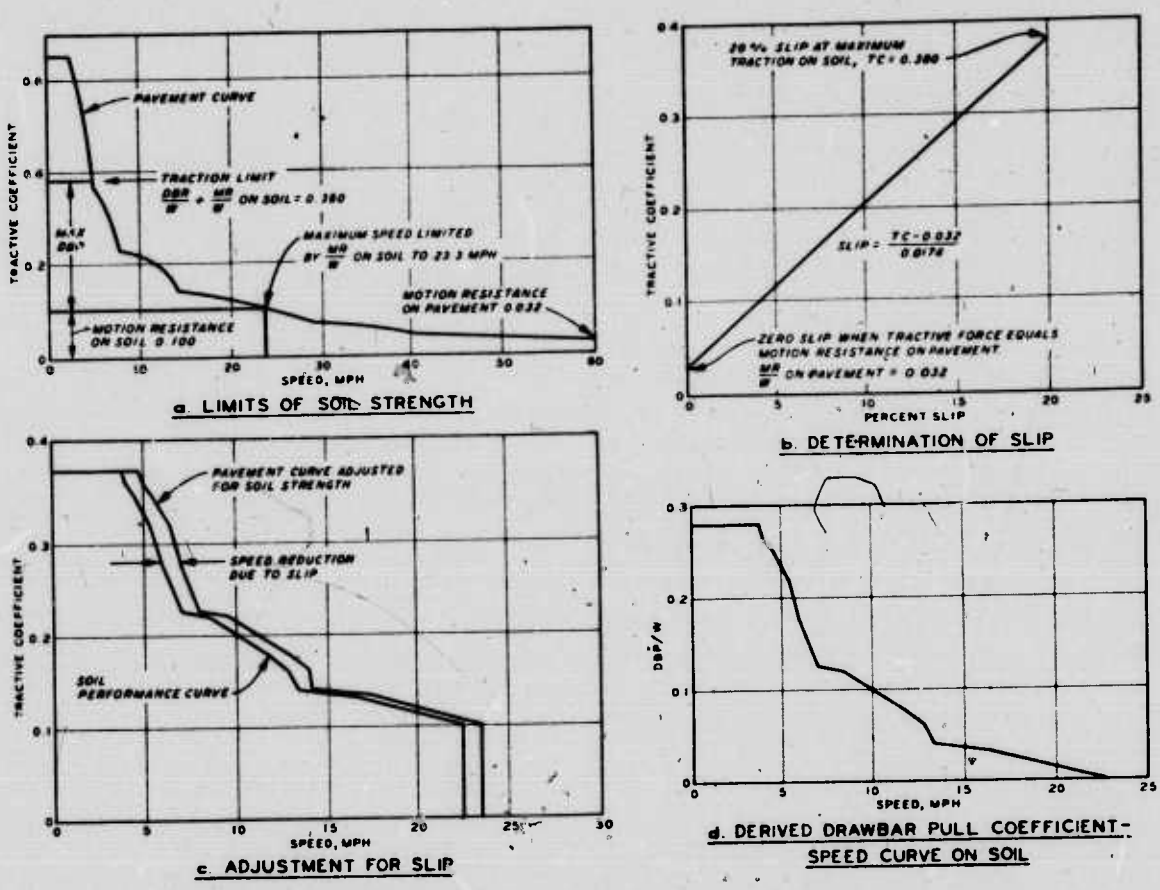

Fig. F14. Determination of soil performance curve and drawbar pull coefficient-speed relations for M35A1 at site 4V-S-3 using the WES curves

for the WES curves method in fig. F14 and table F7. In this example the maximum drawbar pull and motion resistance values used to adjust the pavement curve in plot a, fig. F14, were determined from the WES curves as follows:

a. The VCI_1 for the M35A1 (table F1) was subtracted from the average 0- to 6-in. soil strength for the M35A1 tests at site 4V-S-3 (from table F4) to yield the cone index points above VCI_1; that is, 61 - 31 = 30.

b. The maximum drawbar pull, expressed as DBP/W , was read at 30 CI > VCI_1 from the curves in fig. F13 (q.v., DBP/W = 0.280 when soil strength is 30 CI > VCI_1).

c. The motion resistance coefficient was determined from the

curve in fig. d, plate F3, to be 0.100 for a soil strength of 30 CI > VCI_1 (see paragraph 35).

d. Maximum drawbar pull coefficient and motion resistance were summed to give maximum tractive coefficient on soil (0.280 + 0.100 = 0.380). The values thus obtained were entered on the tractive coefficient axis as shown in plot a, fig. F14, to limit the traction and speed indicated by the pavement curve.

33. To account for the loss of speed as a result of wheel slip, the speeds indicated on the pavement curve (within the limits established by soil strength) were reduced by the percent slip as indicated in plot b, fig. F14, to yield the soil performance curve as shown in plot c, fig. F14. These computations are detailed in table F7. It may be seen that the relation expressed in plot b, fig. F14, shows a 20 percent slip at the maximum tractive coefficient for the M35A1 operating on a soil strength of 61 CI with a linear decay to zero slip at the point where the tractive coefficient equals the motion resistance on pavement as indicated in table F7.

34. The drawbar pull coefficient-speed curve (plot d, fig. F14) was determined by subtracting the motion resistance coefficient (MR/W = 0.100) from the tractive coefficient of the soil performance curve (plot c, fig. F14). The drawbar pull coefficient-speed curve is the basis for the acceleration predictions described in the following paragraphs.

Acceleration predictions

35. In reference 7, Knight demonstrates the use of maximum drawbar pull to determine the capability of a vehicle to climb a slope and to tow another vehicle. The predictions herein are based on the consideration of drawbar pull as the force available to accelerate the vehicle. From this basis the procedures for determining time, distance, and speed for an accelerating vehicle were developed. The following example illustrates the procedure for determining the first increment of velocity change on the drawbar pull coefficient-speed curve (fig. F15). The other increments were handled in a similar manner (table F8).

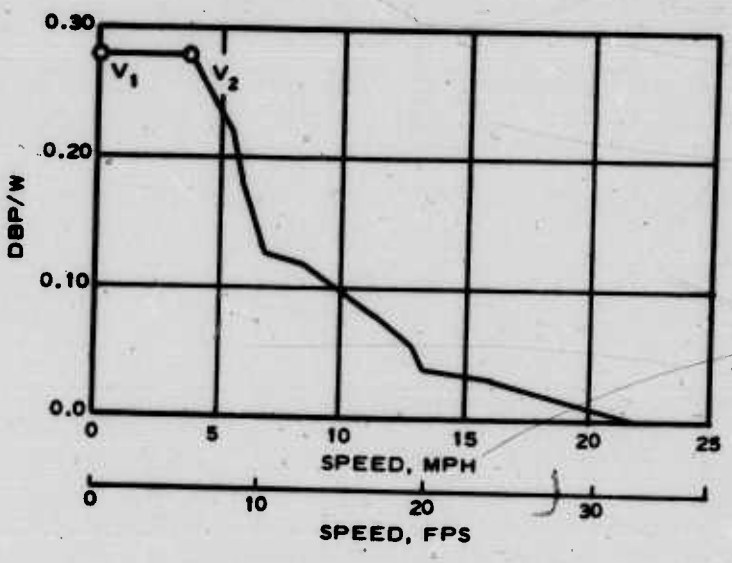

Fig. F15. Drawbar pull coefficient-speed curve for the M35A1 at site 4V-S-3 with the first increment of velocity change indicated

a. The acceleration a from V_1 to V_2 equals the change in velocity divided by the time required to effect the change and may be expressed by equation 1 from paragraph 18:

$$a = \frac{V_2 - V_1}{t} = \frac{5.75 - 0}{t} = \frac{5.75}{t}$$

(V_1 and V_2 are given in feet per second in table F8 for each increment.)

b. The force F required to produce this acceleration is equal to the mass (W/g) of the vehicle times the acceleration.

$$F = \frac{W}{g}\left(\frac{V_2 - V_1}{t}\right) = \frac{W}{g}\left(\frac{5.75}{t}\right) \qquad (5)$$

c. The force available to produce the velocity change from V_1 to V_2 is the average drawbar pull that can be developed from V_1 to V_2.

$$\overline{DBP} = \left(\frac{\frac{DBP_1}{W} + \frac{DBP_2}{W}}{2}\right) W = \left(\frac{0.280 + 0.280}{2}\right) W = 0.280W \qquad (6)$$

$\frac{DBP_1}{W}$ and $\frac{DBP_2}{W}$ are given in table F8 for each increment.

d. The time t_1 required for the force available $\overline{DBP}$ to effect the velocity change is found by substituting the force available $\overline{DBP}$ for force required F in equation 5 and rearranging:

$$\overline{DBP} = \frac{W}{g}\left(\frac{V_2 - V_1}{t}\right) \qquad (7)$$

$$\left(\frac{\overline{DBP}}{W}\right) g = \frac{V_2 - V_1}{t}$$

$$t = \frac{V_2 - V_1}{\left(\frac{\overline{DBP}}{W}\right) g} = \frac{5.75}{9.00} = 0.64 \text{ sec}$$

e. The distance d the vehicle travels in effecting the velocity change from V_1 to V_2 is found by multiplying the time by the average velocity $\bar{V}$:

$$\bar{V} = \frac{V_1 + V_2}{2} = \frac{0 + 5.75}{2} = 2.88 \text{ fps} \qquad (8)$$

$$d = \bar{V}t = 2.88 \times 0.64 = 1.84 \text{ ft} \qquad (9)$$

Values of V_1 , V_2 , $\bar{V}$, DBP_1/W , DBP_2/W , $\overline{DBP}/W$, $DBP/W \times g$, t , d , cumulative time, and cumulative distance for the example (fig. F15) are given in table F8. The computation of the effects of a gear change while the vehicle is accelerating is given in plate F6.

Deceleration predictions

36. As stated in paragraph 18, when the acceleration is a negative value (as when the vehicle is slowing down), it is termed deceleration. The rationale and the method of predicting the speed and distance traveled for a decelerating vehicle are as follows:

a. Using the basic equation $\frac{V_2 - V_1}{t} = -a$, the change in velocity from V_1 to V_2 divided by the time required to

effect that change is the deceleration when $V_1 > V_2$.

b. The force required to produce this deceleration is equal to the mass W/g of the vehicle times the deceleration:

$$F = \frac{W}{g}\left(\frac{V_2 - V_1}{t}\right) \qquad (10)$$

c. The force available to produce this deceleration in the rolling tests (braking force is discussed in paragraph 37) is the motion resistance MR. Substituting into equation 10

$$MR = \frac{W}{g}\left(\frac{V_2 - V_1}{t}\right) \qquad (11)$$

d. Again, from the basic equation $\frac{V_2 - V_1}{t} = -a$, $-a$ may be substituted into equation 11 and the equation rearranged:

$$\frac{MR}{W} \times g = -a \qquad (12)$$

e. Or

$$\frac{MR}{W} = \frac{-a}{g} \qquad (13)$$

f. Speed at the end of any increment of velocity change may be determined by the equation

$$V_2 = V_1 + at \qquad (14)$$

(a may be either positive or negative)

g. When V_1 is equal to zero, equation 14 becomes:

$$V_2 = at = \left(\frac{MR}{W} \times g\right) t \qquad (15)$$

Or for any time increment from $V_1 = 0$

$$V = at = \left(\frac{MR}{W} \times g\right) t \qquad (16)$$

An example of the computations for the prediction herein is given in table F9.

h. The distance d traveled during deceleration was predicted by the general equation for distance while accelerating from zero velocity:

$$d = 1/2\ at^2 = \left(\frac{MR}{W} \times g\right) t \qquad (17)$$

An example of the computations is shown in table F9.

37. The computations made to determine the speed and distance traveled when the vehicle is decelerating by braking are identical to those for when the vehicle is rolling except that a braking force is used in lieu of motion resistance as the force available to decelerate the vehicle. In the predictions herein, braking force was assumed to be equal to the maximum tractive force the vehicle could develop on the soil conditions being tested. This is admittedly a fairly gross assumption; however, the results (paragraphs 40 and following) were reasonable, and the investigation of braking force-vehicle-soil strength relations was beyond the scope of this study.

Average speed predictions

38. When a section of terrain is of sufficient length for the vehicle under consideration to accelerate to its maximum speed (for instance, 22.39 mph for the M35A1 at site 4V-S-3, from table F7 or fig. F15), the average speed is predicted by dividing the length of the terrain section by the sum of the time required for acceleration to maximum speed, the time traveled at the maximum speed, and the time required to decelerate from the maximum speed to the desired speed at the end of the terrain section. In the tests reported herein, the test courses were not of sufficient length for the vehicles to accelerate to maximum speed; therefore, the average speed was predicted by dividing the length of the test course by the sum of the time required to accelerate and the time required to decelerate. The time required to accelerate and the time required to decelerate are determined by establishing the point of intersection at which the speed-distance curves for acceleration and deceleration span a distance equal to

the test length. The point of intersection is established by the simultaneous solution of the equations of the lines representing the increments of acceleration and deceleration wherein the point of intersection occurs. An example of the computations made to predict the speed, distance, and time at the point of intersection of the acceleration and deceleration curves and the determination of the average predicted speed for M35A1 in test 269 R are given in plate F7. Predicted average speeds for the tests considered in this portion of the analysis are given in table F2. As previously stated, it was not possible to make a prediction for all tests. (Note "Remarks" column of table F2.)

39. An example of the measured and predicted performances for M35A1 test 269 R is shown graphically in plate F8. It may be noted in plate F8 that the driver executed the upward gear shifts at speeds very close to those predicted as optimum for gear change. The dashed lines representing the increments wherein gear shifts occurred in the actual tests are used in the plate because the test data did not permit an exact representation of speed during the 1-sec time interval in which the gear shift occurred. It also appears that the 0.4 sec allowed for deceleration during gear change may be too small a time increment. The measured average speed for this test was 9.7 mph and the predicted average speed (using the WES curves) was 10.1 mph. A summary of M35A1 performance data taken during test 269 R is presented in table F10.

Comparison of Measured and Predicted Average Speeds

Wheeled vehicles

40. A comparison of the average speeds predicted using the WES numeric and using the WES curves with the average speed measured for the wheeled vehicle tests is shown in plate F9. From the plate it may be seen that the predicted speeds were generally higher than the measured speeds, although in many cases they were only slightly higher. Several reasons may be advanced to account for the predicted speeds exceeding the measured speeds:

a. The hard-surface performance curves (plate F5) were obtained with vehicles in near-perfect mechanical condition.

There is no assurance that the vehicles used in the tests reported herein were operating at peak efficiency, and any loss in efficiency within the vehicle itself would result in a lower acceleration capability, hence a lower average speed under the conditions tested.

b. The time allowed (0.4 sec) for deceleration during the gear change may be insufficient, and any increase in time allowed for deceleration during the gear change would result in a lower predicted speed.

It would seem desirable that the scope of future test programs of this nature should include tests to determine the mechanical condition and maximum traction capability of the vehicle on pavement and that tests be conducted to better define changes in velocity that occur during gear changes.

41. The deviation of measured average speed from predicted average speed for each prediction is shown in table F2. The average absolute deviations for the predictions made with the WES numeric and the WES curves are shown in the following tabulation:

	Number of Tests			Average Absolute Deviation, mph					
				WES Numeric			WES Curves		
Vehicle	Rolling	Braking	Total	Rolling	Braking	Total	Rolling	Braking	Total
M151	9	7	16	2.6	3.3	3.0	0.7	2.1	1.3
M37	2	2	4	2.0	2.0	2.0	1.1	1.1	1.1
M35A1	7	4	11	1.8	2.5	1.7	1.7	2.7	2.1
All	18	13	31	2.1	2.9	2.4	1.1	2.1	1.5

It can be seen from the tabulation above and from plate F9 that the predictions made using the WES curves were somewhat better than those made using the WES numeric for the M151 and M37, and that the predictions using the WES numeric were slightly better for the M35A1. It can be seen, too, that the deviations in predictions for the M151 and M35A1 tests that involved braking were greater than those for the tests in which the vehicle rolled to a stop. The average deviation for all wheeled vehicle speed predictions was 1.5 mph using the WES curves and 2.4 mph using the WES

numeric. Of the 31 wheeled vehicle tests for which speed predictions could be made, in 20 tests the average speed predicted by using the WES curves was closer to the measured speed than the prediction made using the WES numeric; in 9 tests the average speed predicted using the WES numeric was closer; and in 2 tests deviation was the same. In brief, from plate F9 and from the tabulation above, it would appear that while both the WES numeric and the WES curves are acceptable for a first-generation model, the empirically derived WES curves yield slightly better predictions.

Tracked vehicles

42. A comparison of the average speeds predicted using the WES curves with the speeds measured in the tests with the tracked vehicles is shown in plate F10. (It will be recalled that the WES numeric has not at this time been extended to include tracked vehicles.) From plate F10 it can be seen that all of the predicted speeds were higher than those measured in the tests, and there is appreciable scatter in the M29C data. The factors mentioned in paragraph 40 in regard to the wheeled vehicles are equally applicable to the tracked vehicle tests and predictions. The average absolute deviations in predicted speeds for the tracked vehicles are shown in the following tabulation:

Vehicle	Number of Tests			Average Absolute Deviation mph		
	Rolling	Braking	Total	Rolling	Braking	Overall
M29C	10	4	14	2.7	3.8	3.0
M113	5	2	7	1.7	1.6	1.7
Both	15	6	21	2.3	3.1	2.6

It can be seen that the average deviation for the M113 predictions was much smaller than the average deviation for the M29C predictions. When it is considered that the M29C used in these tests was approximately 20 years older than the M113, these data do seem to emphasize the need to establish the maximum traction capability of the test vehicles on a firm surface.

PART IV: CONCLUSIONS AND RECOMMENDATIONS

Conclusions

43. Based on the analysis of the data presented herein and subject to the limitations imposed by these data, the following conclusions are offered:

a. Performance of wheeled and tracked vehicles in soft clay soils in terms of acceleration can be related to soil strength expressed as the average 0- to 6-in. cone index; however, the data secured in this program do not permit defining the relation (paragraphs 21 and 22).

b. Performance of wheeled and tracked vehicles in soft clay soils in terms of deceleration can be correlated empirically with soil strength expressed as the average 0- to 6-in. cone index. While the data collected in this program do not permit a complete development of the relation, logical extrapolations can be made (paragraphs 25 and 26).

c. While both the empirical WES curves and the semiempirical WES numeric appear to adequately define the drawbar pull coefficient-soil strength and motion resistance-soil strength relations for use in a first-generation model the WES curves permitted a slightly more accurate prediction of average speed for the tests reported herein (paragraph 41).

Recommendations

44. It is recommended that:

a. Additional studies be conducted to improve and extend the relations presented in this report.

b. Additional studies be conducted to establish other relations and/or input parameters needed for the WES analytical model such as are posed by the following questions:

(1) What is the peak performance of the vehicle?

(2) Does time required to shift gears vary with transmission type and vehicle, and if so, to what magnitude?

(3) Does braking force vary with speed, with soil strength, or with surface condition, and to what magnitude?

(4) At what limiting slip can the driver still maintain adequate control of the vehicle, and does this vary with speed?

LITERATURE CITED

1. Rula, A. A. et al., "Relative Off-Road Performance of the M60A1E1 and MBT-70 Tanks" (in preparation), U. S. Army Engineer Waterways Experiment Station, CE, Vicksburg, Miss.

2. Benn, B. O. and Keown, M., "An Analytical Model for Predicting Cross-Country Vehicle Performance; Appendix A: Instrumentation of Test Vehicles," Technical Report No. 3-783, July 1967, U. S. Army Engineer Waterways Experiment Station, CE, Vicksburg, Miss.

3. Freitag, D. R., "A Dimensional Analysis of the Performance of Pneumatic Tires on Soft Soils," Technical Report No. 3-688, Aug 1965, U. S. Army Engineer Waterways Experiment Station, CE, Vicksburg, Miss.

4. Richmond, L. D. et al., "Aircraft Dynamic Loads from Substandard Landing Sites; Part II: Development of Tire-Soil Mathematical Model," Technical Report AFFDL-TR-67-145, Sept 1968, Air Force Flight Dynamics Laboratory, Air Force Systems Command, Wright-Patterson Air Force Base, Ohio.

5. Smith, J. L., "A Study of the Effects of Wet Surface Soil Conditions on the Performance of a Single Pneumatic-Tired Wheel," Technical Report No. 3-703, Nov 1965, U. S. Army Engineer Waterways Experiment Station, CE, Vicksburg, Miss.

6. Blackmon, C. A., Stinson, B. G., and Stoll, J. K., "An Analytical Model for Predicting Cross-Country Vehicle Performance; Appendix D: Performance of Amphibious Vehicles in the Water-Land Interface (Hydrologic Geometry)," Technical Report No. 3-783, Feb 1970, U. S. Army Engineer Waterways Experiment Station, CE, Vicksburg, Miss.

7. Knight, S. J., "Trafficability of Soils; A Summary of Trafficability Studies Through 1955," Technical Memorandum No. 3-240, 14th Supplement, Dec 1956, U. S. Army Engineer Waterways Experiment Station, CE, Vicksburg, Miss.

8. Depkin, R. F., "Wheeled Vehicle Performance Data Consolidation," Report No. DPS-2410, June 1967, Aberdeen Proving Ground, Md.

Table F1

Pertinent Vehicle Characteristics

Vehicle	Test Weight lb	Engine			Ground Clearance in.	Tire						VCI_1*
		Type	Brake HP	Transmission		Size	Ply Rating	Width in.	Section Height in.	Diameter in.	Deflection in.	
M151	3,080	Gasoline	71	Manual syncromesh	10.3	7.00-16	6	8.7	6.038	30.22	1.76	21
M37	7,470	Gasoline	78	Manual syncromesh	11.0	9.00-16	8	12.2	8.585	35.7	3.40	23
M35A1	19,315	Multifuel	146	Manual syncromesh	12.5	11.00-20	8	12.9	10.22	40.44	3.20	31

Vehicle	Test Weight lb	Engine			Ground Clearance in.	Track					VCI_1*
		Type	Brake HP	Transmission		Contact Length in.	Width in.	Shoe in.	Contact Pressure psi	Bogies in Contact with Ground Each Side	
M29C	6,020	Gasoline	65	Manual	11.0	78	20	4.5	1.9	8	9
M113	22,073	Gasoline	215	Hydraulic	16.1	105	15	6.0	7.0	5	13

* VCI_1 = the minimum soil strength required for a vehicle to complete one pass on a level surface.

Table F2

Summary of Vehicle Performance Data and Speed Predictions

Site	Code No.	Test No. and Type	Length ft	Time sec	Acceleration while Rolling ft/s²	Deceleration while Braking ft/s²	Deceleration while Braking ft/s²	Average Speed, mph: Measured	Predicted on Basis of: Numeric	Predicted on Basis of: WES Curves	Deviation of Predicted Speed, mph: Numeric	Deviation of Predicted Speed, mph: WES Curves	Remarks
								M151					
MV-8-3	2	292 R	*	*	0.453	0.119		*	*	*	*	*	Distance play-out too short for test
	4	294 R	283.7	16.6	0.441	0.103		11.7	6.3	12.6	-5.4	+0.9	
	5	296 B	254.5	10.8	0.559		0.396	16.1	19.6	16.9	+3.5	+0.8	Revolutions count invalid after 8 sec
MRDC-X_{10}	5	286 R	281.5	16.1	0.286	0.146		11.9	8.1	12.4	-3.8	+0.5	
	6	287 R	282.0	16.0	0.280	0.140		12.0	8.1	12.4	-3.9	+0.4	
	7	290 R	227.5	14.6	0.255	0.133		10.6	7.3	11.2	-3.3	+0.6	
	8	289 B	244.9	13.0	0.292		0.397	12.8	17.9	16.1	+5.1	+3.3	Revolutions count invalid after 11 sec
	9	291 B	251.0	12.4	0.267		0.366	13.8	18.1	16.2	+4.3	+2.4	Revolutions count invalid after 10 sec
MRDC-X_2	10	297 R	136.5	*	0.211	0.149		*	*	*	*	*	Distance play-out invalid after 13 sec
	11	298 R	157.5	12.5	0.255	0.148		8.6	7.5	9.7	-1.1	+1.1	
	12	299 R	157.2	12.0	0.304	0.166		9.0	7.5	9.7	-1.5	+0.7	
	13	300 B	169.9	11.1	0.287		0.370	10.2	13.5	12.9	+3.3	+2.7	Revolutions count invalid for last second
	14	301 B	168.0	10.4	0.373		0.193	10.6	13.4	12.8	+2.8	+2.2	Revolutions count invalid after 8 sec
MRDC-X_4	15	302 R	286.7	16.1	0.317	0.130		12.1	10.5	12.7	-1.6	+0.6	
	16	303 R	248.7	15.0	0.280	0.121		11.3	9.8	11.9	-1.5	+0.6	
	17	304 R	249.0	15.0	0.317	0.125		11.3	9.8	11.9	-1.5	+0.6	
	18	305 B	241.7	13.1	0.323		0.297	12.6	15.2	14.5	+2.6	+1.9	Revolutions count invalid after 10 sec
	19	306 B	179.1	11.0	0.217		0.323	11.1	13.2	12.7	+2.1	+1.6	Revolutions count invalid after 9 sec
								M37					
MV-8-3	20	260 R	*	*	0.224	0.108		*	*	*			Distance play-out invalid after 8 sec
	21	261 R	247.0	15.7	0.273	0.116		10.7	8.1	10.4	-2.6	-0.3	Revolutions count invalid after 10 sec
	22	262 R	*	*	0.230	0.113		*	*	*	*	*	Distance play-out invalid after 10 sec
	23	263 B	269.7	14.5	0.211		0.286	12.7	15.1	10.8	+2.4	-1.9	Revolutions count invalid after 10 sec
	24	264 B	268.3	13.4	0.261		0.280	13.2	14.9	12.9	+1.7	-0.3	Revolutions count invalid after 11 sec
MRDC-X_{10}	25	206 R	*	*	0.236	0.116		*	*	*	*	*	Distance play-out invalid after 14 sec
	26	212 R	*	*	0.168	0.123		*	*	*	*	*	Distance play-out invalid after 15 sec
	27	215 R	*	*	0.161	0.114		*	*	*	*	*	Distance play-out too short for test
	28	209 B	244.2	19.6	0.248		0.193	8.5	*	*	*	*	Driver released brakes
	29	214 B	*	*	0.161		*	*	*	*	*	*	Revolutions count and distance play-out invalid after 11 sec
	30	210 B	*	*	0.211		0.373	*	*	*	*	*	Revolutions count and distance play-out invalid after 13 sec
MRDC-X_2	31	318 R	*	*	0.140	0.122			*	*			Distance play-out invalid after 16 sec
	32	320 R	221.9	19.0	0.143	0.118		8.0	9.5	9.9	+1.5	+1.9	
	33	321 R	213.5	20.0	*	*		7.3	*	*	*	*	Tire flat when test was run
MRDC-X_4	34	316 R	*	*	0.118	0.121		*	*	*	*	*	Rolling start; test length unknown
	35	317 R	*	*	0.099	0.132		*	*	*	*	*	Distance play-out invalid after 14 sec

(Continued)

* Data not available.

Table F2 (Concluded)

Site	Code No.	Test No. and Type	Length ft	Time sec	Acceleration a/g	Deceleration While Rolling -a/g	Deceleration While Braking -a/g	Average Speed, mph: Measured	Predicted on Basis of: Numeric	Predicted on Basis of: WES Curves	Deviation of Predicted Speed, mph: Numeric	Deviation of Predicted Speed, mph: WES Curves	Remarks
								M35A1					
4V-S-3	36	265 R	243.1	19.0	0.304	0.087		8.7	9.3	9.9	+0.6	+1.2	Revolutions count invalid after 18 sec
	37	267 R	243.9	18.1	0.342	0.094		9.2	9.3	10.2	+0.1	+0.1	
	38	269 R	270.3	19.0	0.224	0.098		9.7	9.8	10.1	+0.1	+0.4	Revolutions count invalid after 12 sec
	39	266 B	224.1	14.6	0.280		0.245	10.5	12.4	11.9	+1.9	+1.4	Revolutions count invalid after 12 sec
	40	268 B	250.8	16.0	0.354		0.252	10.7	12.9	12.4	+2.2	+1.7	Revolutions count invalid after 14 sec
MRDC-X_{10}	41	292 R	219.1	20.2	0.161	0.103		7.4	9.3	9.8	+1.9	+2.4	
	42	293 R	248.7	22.3	0.149	0.093		7.6	9.7	10.2	+2.1	+2.6	
	43	295 B	212.2	19.0	0.149		0.329	7.6	10.4	11.2	+2.8	+3.6	Revolutions count invalid after 17 sec
	44	296 B	215.5	20.0	0.161		0.289	7.3	10.5	11.3	+3.2	+4.0	Revolutions count invalid after 18 sec
MRDC-X_2	45	322 R	72.3	13.3	0.087			3.7	5.4	5.6	+1.7	+1.9	Front-wheel drive disengaged
	46	323 R	165.2	23.2	0.118	0.107		4.9	7.2	7.2	+2.3	+2.3	
								M2AC					
4V-S-3	47	276 R	246.0	18.0	0.234	0.085		9.3		10.4		+1.1	
	48	277 R	253.0	17.5	0.279	0.099		9.9		10.5		+0.6	
	49	278 B	266.0	15.5	0.276		0.255	11.7		13.4		+1.7	
MRDC-X_{10}	50	282 R	187.0	22.0	0.124	0.106		5.8		9.3		+3.5	
	51	284 R	232.5	26.5	0.186	0.095		6.0		10.2		+4.2	
	52	285 B	235.2	26.4	0.118		0.149	6.1		10.2		+4.1	
MRDC-X_4	53	307 R	232.6	21.0	0.161	0.100		7.6		10.2		+2.6	
	54	308 R	234.0	20.5	0.152	0.109		7.8		10.2		+2.4	
	55	309 R	233.0	20.5	0.205	0.112		7.7		10.2		+2.5	
	56	310 B	216.6	21.1	0.155		0.233	7.0		12.1		+5.1	
	57	311 B	189.5	18.3	0.161		0.193	7.1		11.6		+4.5	
MRDC-X_6	58	312 R	210.6	22.2	0.118	0.121		6.5		9.3		+2.8	
	59	313 R	207.3	24.9	0.168	0.124		5.7		9.2		+3.5	
	60	314 R	208.0	25.1	0.112	0.099		5.6		9.2		+3.6	
								M113					
4V-S-3	61	270 R	311.8	20.9	0.199	0.099		10.2		11.6		+1.4	Instrumentation malfunction
	62	271 R	248.0	17.9	*	*		9.4		10.6		+1.2	
	63	273 R	249.5	17.8	0.242	0.089		9.6		10.6		+1.0	
	64	272 B	221.5	13.0	*		*	11.6		13.0		+1.4	
	65	274 B	232.5	13.8	0.230		0.171	11.5		13.2		+1.7	
MRDC-X_2	66	324 R	177.3	17.5	0.186	0.085		6.9		9.3		+2.4	
	67	325 R	164.2	17.0	0.115	0.099		6.6		8.9		+2.3	

* Data not available.

Table F3

Summary of Soil Classification Data

Test Area	Site	Depth in.	Percent Fines	Atterberg Limits LL	PL	PI	USCS Soil Type
Pran Buri	4V-S-3	0-6	90	70	25	45	CH
		6-12	89	64	23	41	CH
Phet Buri	MRDC-X_{10}	0-6	98	51	24	27	CH
		6-12	99	56	25	31	CH
Samut Prakan	MRDC-X_2	0-6	97	81	29	52	CH
		6-12	97	73	26	47	CH
	MRDC-X_4	0-6	99	76	29	47	CH
		6-12	98	85	29	56	CH
	MRDC-X_6	0-6	97	102	33	69	CH
		6-12	99	149	35	114	CH

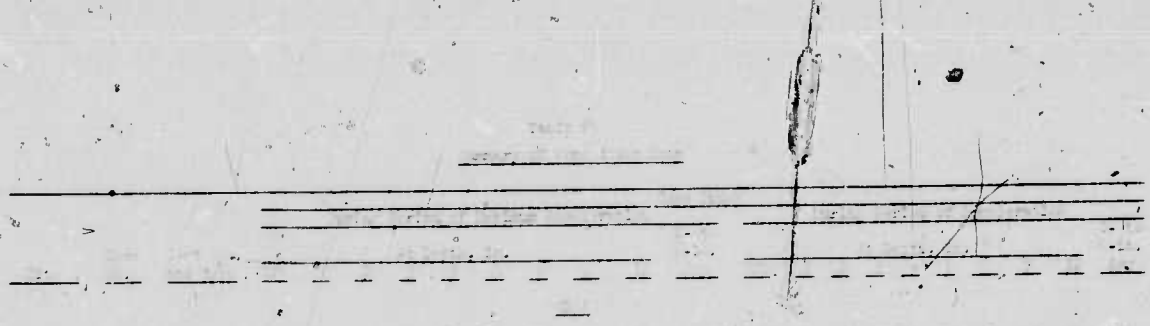

Table [illegible]

Summary of Data for Tractive Coefficient-Speed Curves on Pavement

M151 Speed mph	M151 Tractive Coefficient	M37 Speed mph	M37 Tractive Coefficient	M35A1 Speed mph	M35A1 Tractive Coefficient	M29C Speed mph	M29C Tractive Coefficient	M113 Speed mph	M113 Tractive Coefficient
[illegible]	0.805	0.0	0.857	0.0	0.649	0.0	0.817	0.0	0.815
[illegible]	[illegible]	[illegible]	0.857	[illegible]	0.649	[illegible]	0.817	1.7	0.715
[illegible]	0.780	[illegible]	0.836	[illegible]	[illegible]	[illegible]	0.812	1.8	[illegible]
7.0	[illegible]	[illegible]	0.8[illegible]1	[illegible]	0.473	[illegible]	[illegible]	[illegible]	[illegible]
[illegible]	[illegible]	[illegible]	0.790	[illegible]	0.369	[illegible]	0.608	[illegible]	0.506
9.0	[illegible]	[illegible]	0.74[illegible]	[illegible]	0.35[illegible]	[illegible]	[illegible]	[illegible]	0.43[illegible]
10.0	[illegible]	[illegible]	0.710	[illegible]	0.319	[illegible]	0.585	[illegible]	0.390
10.7	[illegible]	[illegible]	0.671	[illegible]	0.278	[illegible]	0.581	[illegible]	[illegible]
[illegible]	[illegible]	[illegible]	[illegible]	[illegible]	0.227	5.0	[illegible]	[illegible]	[illegible]
[illegible]	[illegible]	[illegible]	0.460	[illegible]	[illegible]	5.5	[illegible]	[illegible]	[illegible]
14.0	[illegible]	[illegible]	[illegible]	[illegible]	0.177	6.0	0.515	[illegible]	[illegible]
[illegible]	[illegible]	[illegible]	[illegible]	[illegible]	0.16[illegible]	[illegible]	[illegible]	12.0	0.156
16.0	0.399	6.0	[illegible]	[illegible]	0.141	7.0	[illegible]	13.7	[illegible]
17.0	0.38[illegible]	[illegible]	0.410	17.5	0.13[illegible]	7.5	0.411	16.0	0.151
18.0	0.370	[illegible]	[illegible]	[illegible]	0.100	8.0	0.365	18.1	0.14[illegible]
19.0	[illegible]	[illegible]	0.391	[illegible]	[illegible]	[illegible]	0.340	20.0	0.12[illegible]
[illegible]	0.300	[illegible]	0.367	[illegible]	[illegible]	9.0	0.334	21.3	0.115
20.5	[illegible]	[illegible]	[illegible]	[illegible]	[illegible]	9.5	0.328	[illegible]	[illegible]
20.7	[illegible]	9.9	[illegible]	40.0	[illegible]	10.0	0.311	[illegible]	0.080
21.0	[illegible]	[illegible]	[illegible]	[illegible]	[illegible]	10.5	0.301	[illegible]	0.078
22.0	[illegible]	14.1	[illegible]	[illegible]	0.047	11.0	0.270	[illegible]	0.073
23.0	[illegible]	14.1	0.13[illegible]	53.0	0.041	11.5	0.241	[illegible]	0.06[illegible]
24.0	[illegible]	[illegible]	0.127	57.4	0.036	12.0	[illegible]	40.0	[illegible]
25.0	0.240	[illegible]	0.103	60.0	0.03[illegible]	[illegible]	0.178		
26.0	0.237	[illegible]	[illegible]			13.0	0.174		
27.0	0.233	[illegible]	0.055			14.0	0.169		
28.0	0.230	40.0	0.040			15.0	0.164		
29.0	0.226					16.0	0.159		
30.0	0.222					17.0	0.154		
30.0	0.218					18.0	0.149		
34.0	0.202								
36.0	0.194								
38.0	0.184								
40.0	0.170								

Note: M151 and M37 data from reference 8. M35A1 and M113 data from WES field tests 2-3 July 1968 (unpublished). M29C data from WES field tests 25 March 1965 (unpublished).

Table 36

Summary of Data Used to Predict Vehicle Performance

Site	Average Cone Index	WES Numeric	WES Numeric				WES Curves			
			60 Drawbar Pull		Motion Resistance		Drawbar Pull		Motion Resistance	
			lb	Coefficient	lb	Coefficient	lb	Coefficient	lb	Coefficient
M151										
4V-S-3	61	11.2	1472	0.478	58	0.019	924	0.30	308	0.10
MRDC-X_{10}	46	8.5	1152	0.374	102	0.033	832	0.27	308	0.10
MRDC-X_2	35	6.4	824	0.274	163	0.053	706	0.23	394	0.115
MRDC-X_4	31	5.7	727	0.236	197	0.064	616	0.20	385	0.125
M37										
4V-S-3	58	7.6	2794	0.374	299	0.040	2166	0.29	747	0.10
MRDC-X_{10}	50	6.6	2121	0.284	374	0.050	2017	0.27	747	0.10
MRDC-X_2	35	4.7	1322	0.177	642	0.086	1643	0.22	896	0.12
MRDC-X_4	30	4.0	947	0.131	822	0.110	1270	0.17	971	0.13
M35A1										
4V-S-3	61	15.5	4346	0.225	1294	0.067	5408	0.28	1931	0.10
MRDC-X_{10}	46	4.2	2801	0.145	1970	0.102	4339	0.235	2125	0.11
MRDC-X_2	34	3.1	1294	0.067	3129	0.162	1543	0.08	3477	0.18
M29C										
4V-S-3	58						1836	0.305	572	0.095
MRDC-X_{10}	52						1746	0.290	572	0.095
MRDC-X_4	30						1258	0.209	602	0.100
MRDC-X_6	18						771	0.128	662	0.110
M113										
4V-S-3	61						6666	0.302	2097	0.095
MRDC-X_2	42						5386	0.244	2163	0.098

Table F7

Determination of Soil Performance Curve for M35A1 at Site 4V-S-3

Tractive Coefficient*	Hard Surface Speed,* mph	Slip** %	Speed on Soil, mph	Drawbar Coefficient
0.649	0.0			
0.649	2.5			
0.582	3.5			
0.473	4.5			
0.380+	4.9	20.00	3.92	0.280
0.365	5.0	19.14	4.04	0.265
0.355	5.5	18.56	4.48	0.255
0.319	6.5	16.50	5.43	0.219
0.278	7.0	14.14	6.01	0.178
0.227	8.0	11.21	7.10	0.127
0.221	9.5	10.86	8.46	0.121
0.177	13.0	8.33	11.91	0.077
0.162	14.0	7.47	12.95	0.062
0.141	14.2	6.26	13.31	0.041
0.132	17.5	5.75	16.49	0.032
0.100++	23.3	3.91	22.39	0.000
0.093	25.0			
0.072	29.0			
0.066	34.6			
0.051	40.0			
0.049	46.5			
0.047	49.5			
0.041	53.0			
0.036	57.4			
0.032‡	60.0			

* From table F5.

** From fig. F14, slip = $\frac{TC - 0.032}{0.0174}$

\+ $\frac{DBP}{W} + \frac{MR}{W}$ from table F6.

++ $\frac{MR}{W}$ from table F6.

‡ $\frac{MR}{W}$ on pavement from table F5.

Example:

Speed on hard surface - slip = speed on soil

or $4.9\left(1 - \frac{20}{100}\right) = 3.92$

Table F8

Computation of Predicted Acceleration Data for M35A1 at Site 4V-S-3

V_1 fps	V_2 fps	$\bar{V}$ fps	$\frac{DBP_1}{W}$	$\frac{DBP_2}{W}$	$\frac{\overline{DBP}}{W}$	$\left(\frac{\overline{DBP}}{W}\right)g$	Time (t) sec	Distance (d) ft	Cumulative Time sec	Cumulative Distance ft	V_2 mph
0.00	5.75	2.88	0.280	0.280	0.280	9.00	0.64	1.84	0.64	1.84	3.92
5.75	5.93	5.84	0.280	0.265	0.272	8.75	0.02	0.12	0.66	1.96	4.04
5.93	6.57	6.25	0.265	0.255	0.260	8.36	0.08	0.50	0.74	2.46	4.48
6.57	7.96	7.26	0.255	0.219	0.237	7.62	0.18	1.31	0.92	3.77	5.43
7.96	8.81	8.38	0.219	0.178	0.198	6.37	0.13	1.09	1.05	4.86	6.01
8.81	10.41	9.61	0.178	0.127	0.152	4.89	0.33	3.17	1.38	8.03	7.10
10.41	9.12*	9.77	--	--	0.100	3.22	0.40	3.91	1.78	11.94	6.22
9.12	10.41	9.77	--	0.127	0.127	4.08	0.32	3.12	2.10	15.06	7.10
10.41	12.41	11.41	0.127	0.121	0.124	3.99	0.50	5.70	2.60	20.76	8.46
12.41	17.47	14.94	0.121	0.077	0.099	3.18	1.59	23.75	4.19	44.51	11.91
17.47	18.99	18.23	0.077	0.062	0.070	2.25	0.68	12.40	4.87	56.91	12.94
18.99	17.70**	18.34	--	--	0.100	3.22	0.40	7.34	5.27	64.25	11.91
17.70	18.99	18.34	--	0.062	0.062	1.99	0.65	11.92	5.92	76.17	12.95
18.99	19.52	19.26	0.062	0.041	0.052	1.67	0.32	6.16	6.24	82.33	13.31
19.52	24.18	21.85	0.041	0.032	0.036	1.16	4.02	87.84	10.26	170.17	16.49†
24.18	32.84	28.51	0.032	0.000	0.016	0.51	16.98	484.10	27.24	654.27	22.39††

Note: V_1 = speed at beginning of increment; V_2 = speed at end of increment; $\bar{V}$ = average speed for increment — Converted to feet per second from $\frac{DBP}{W}$-speed curve, fig. F15, and table F7.

$\frac{DBP_1}{W}$ = maximum drawbar pull/weight at speed V_1; $\frac{DBP_2}{W}$ = maximum drawbar pull/weight at speed V_2 — From $\frac{DBP}{W}$-speed curve, fig. F15, and table F7.

Equations:

$$\bar{V} = \frac{V_1 + V_2}{2} \qquad \frac{\overline{DBP}}{W} = \frac{\frac{DBP_1}{W} + \frac{DBP_2}{W}}{2} \qquad t = \frac{V_2 - V_1}{\frac{\overline{DBP}}{W} \times g} \qquad d = \bar{V}t$$

* Gear change, see plate F6.
** Gear change.
† Point A, plate F7.
†† Point B, plate F7.

Table F9

Computation of Predicted Deceleration Data for M35A1 at Site 4V-S-3

Time sec	$\frac{MR}{W}$	$\left(\frac{MR}{W}\right) g$ ft/sec^2	Speed fps	Speed mph	Distance ft	Test Length ft	Distance from Beginning of Test, ft
0	0	0.000	0.00	0.00	0.00	270.3	270.30
1	0.100	3.216	3.22	2.19	1.61	270.3	268.69
2	0.100	3.216	6.43	4.39	6.43	270.3	263.87
3	0.100	3.216	9.65	6.59	14.47	270.3	255.83
4	0.100	3.216	12.86	8.77	25.73	270.3	244.57
5	0.100	3.216	16.08	10.96	40.20	270.3	230.10
6	0.100	3.216	19.30	13.16	57.89	270.3	212.41
7	0.100	3.216	22.51	15.35	78.79	270.3	191.51*
8	0.100	3.216	25.73	17.54	102.91	270.3	167.39**
9	0.100	3.216	28.94	19.73	130.25	270.3	140.05
10	0.100	3.216	32.16	21.93	160.80	270.3	109.50

Example:

For Speed at 5 Sec

$V = at$

$V = \left(\frac{MR}{W} \times g\right)t$

$V = 3.216(5)$

$V = 16.08$

16.08 fps = 11.0 mph

For Distance at 5 Sec

$d = \frac{1}{2} at^2$

$d = \frac{1}{2}\left(\frac{MR}{W} \times g\right)t^2$

$d = \frac{1}{2}(3.216)(5)^2$

$d = 40.20$ ft

270.3 - 40.20 = 230.10 ft from beginning of test

* Point C, plate F7.
** Point D, plate F7.

Table F10

Summary of M35A1 Performance Data for Test 269 R

Time, sec		Distance, ft		Average Speed	
Start of Increment	End of Increment	Start of Increment	End of Increment	fps	mph
0	1	0.0	3.6	3.6	2.5
1	2	3.6	13.3	9.7	6.6
2	3	13.3	23.8	10.5	7.2
3	4	23.8	36.7	12.9	8.8
4	5	36.7	52.8	16.1	11.0
5	6	52.8	71.1	18.3	12.5
6	7	71.1	91.1	20.0	13.6
7	8	91.1	110.7	19.6	13.0
8	9	110.7	131.4	20.4	13.9
9	10	131.4	152.4	21.3	14.5
10	11	152.4	174.6	22.2	15.1
11	12	174.6	197.1	22.5	15.3
12	13	197.1	217.6	20.5	14.0
13	14	217.6	234.6	17.0	11.6
14	15	234.6	247.3	12.7	8.7
15	16	247.3	257.2	9.9	6.7
16	17	257.2	264.3	7.1	4.8
17	18	264.3	268.7	4.4	3.0
18	19	268.7	270.3	1.6	1.1

BLANK PAGE

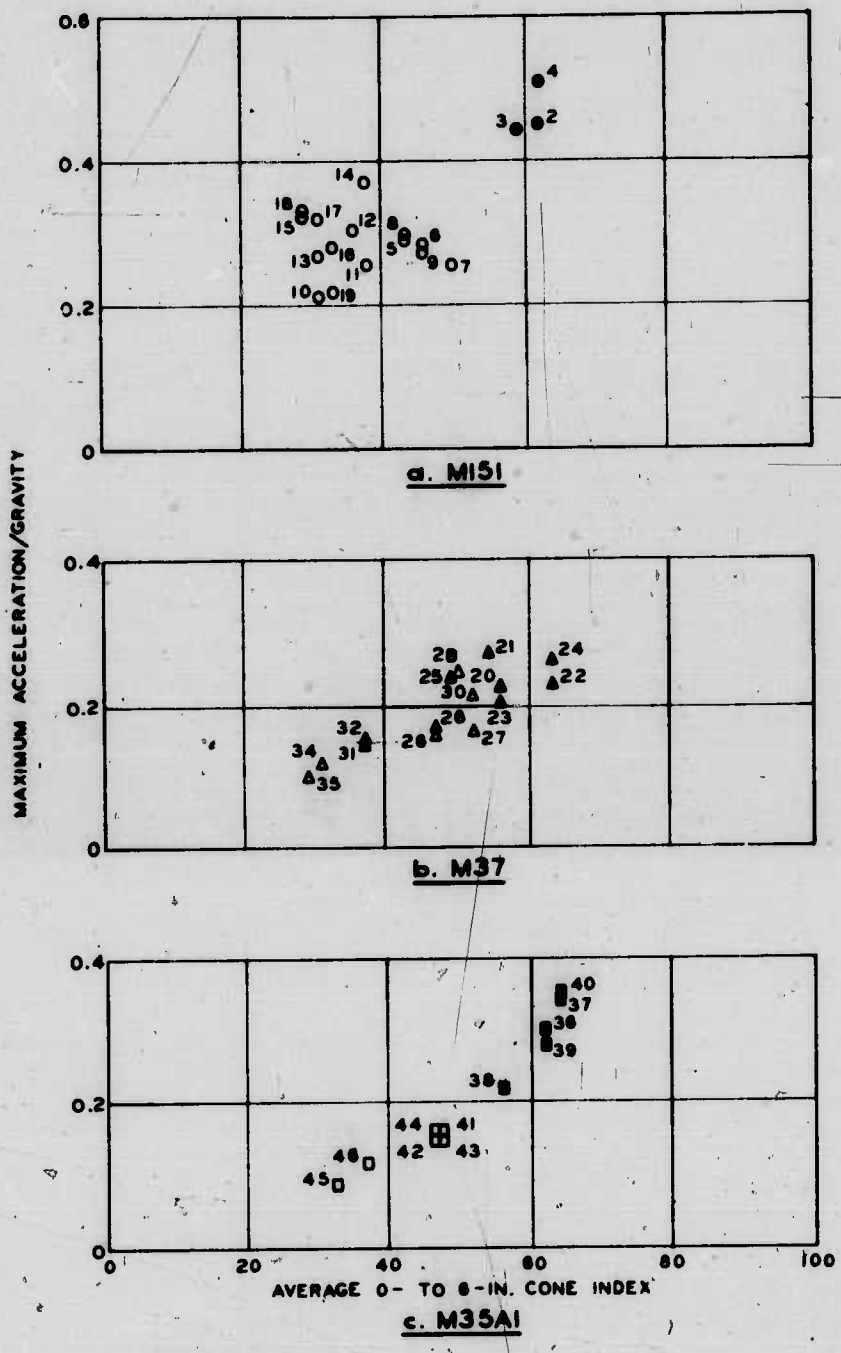

LEGEND

OPEN SYMBOLS INDICATE BARE SURFACES.
CLOSED SYMBOLS INDICATE GRASS-COVERED SURFACES.
NUMBERS NEAR PLOTTED POINTS ARE CODE NUMBERS FROM TABLES F2 AND F4.

ACCELERATION RELATIONS FOR WHEELED VEHICLES

PLATE F1

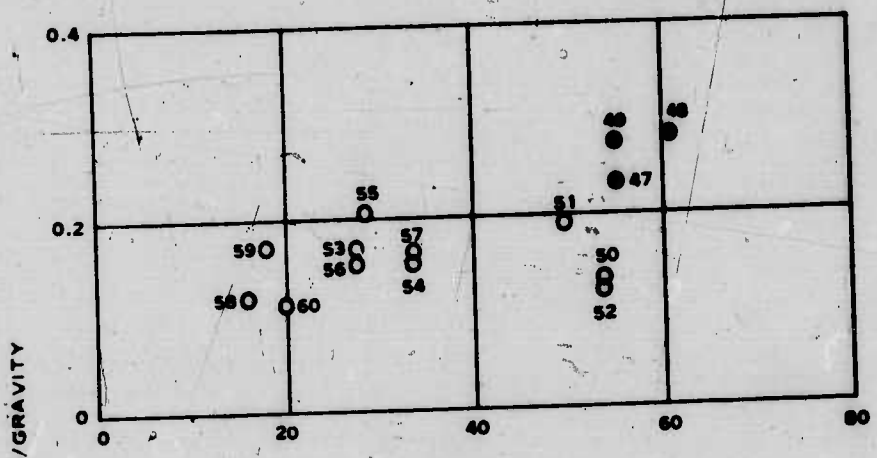

a. M29C

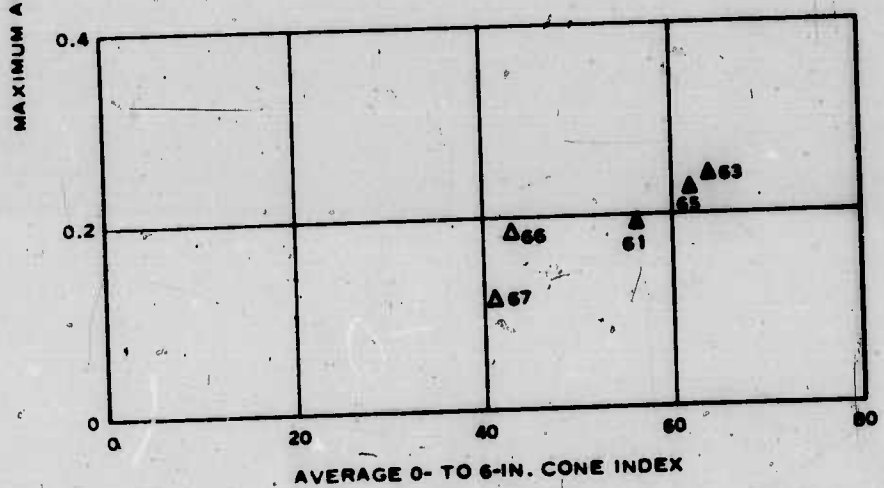

b. M113

LEGEND

OPEN SYMBOLS INDICATE BARE SURFACES

CLOSED SYMBOLS INDICATE GRASS-COVERED SURFACES

NUMBERS NEAR PLOTTED POINTS ARE CODE NUMBERS FROM TABLES F2 AND F4

ACCELERATION RELATIONS FOR TRACKED VEHICLES

PLATE F2

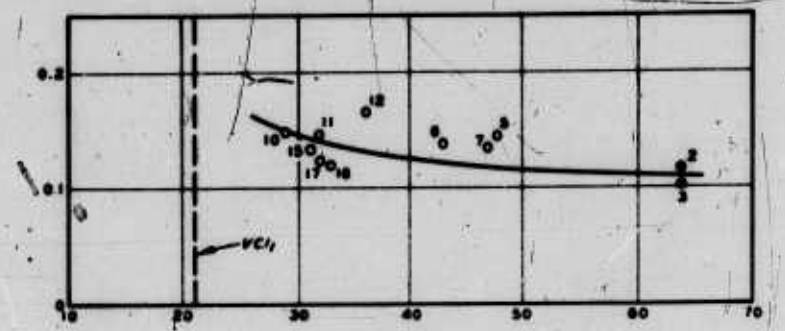

a. M151

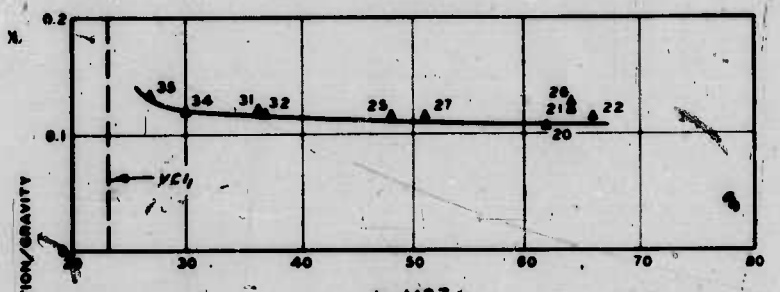

b. M37

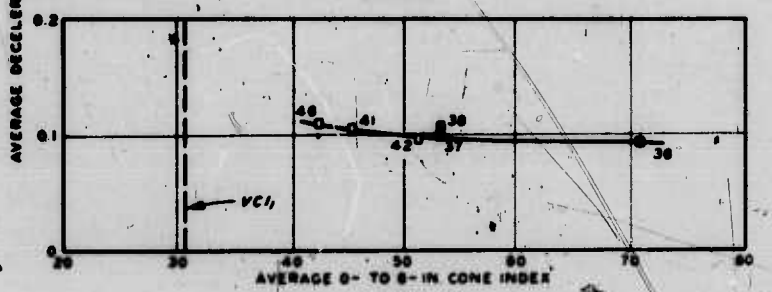

c. M35A1

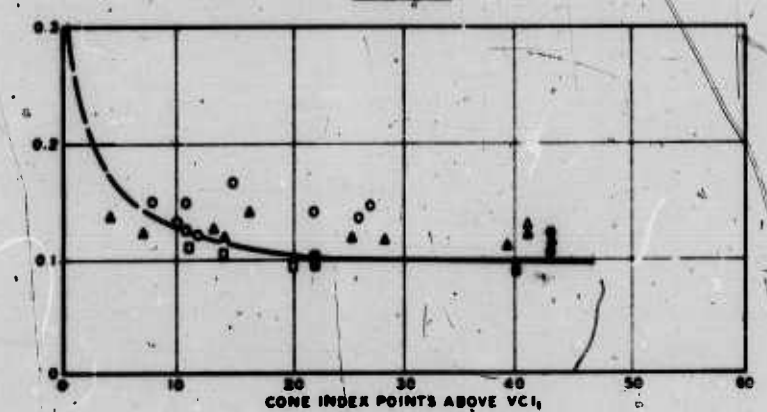

d. SUMMARY

LEGEND

OPEN SYMBOLS INDICATE BARE SURFACES.
CLOSED SYMBOLS INDICATE GRASS-COVERED SURFACES.
NUMBERS NEAR PLOTTED POINTS ARE CODE NUMBERS FROM TABLES F2 AND F4

DECELERATION RELATIONS FOR WHEELED VEHICLES

PLATE F3

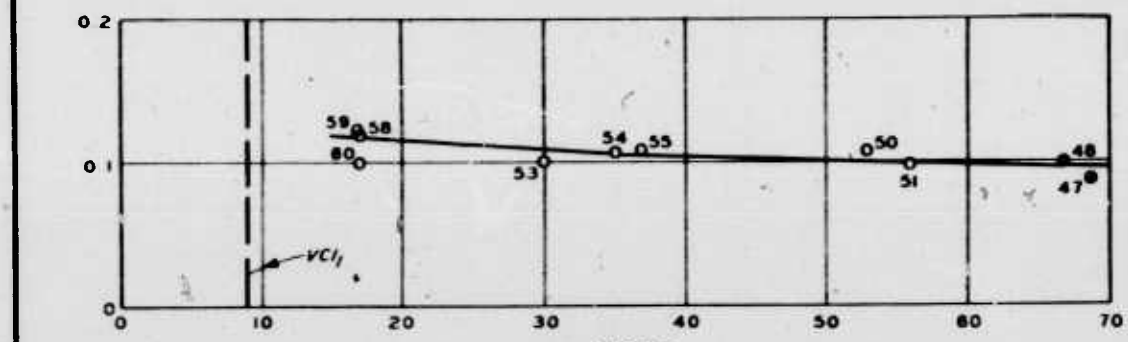

a. M29C

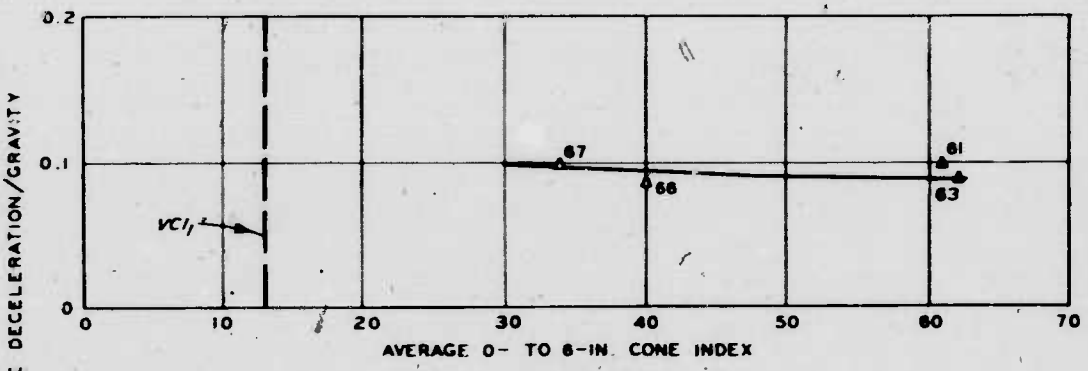

b. M113

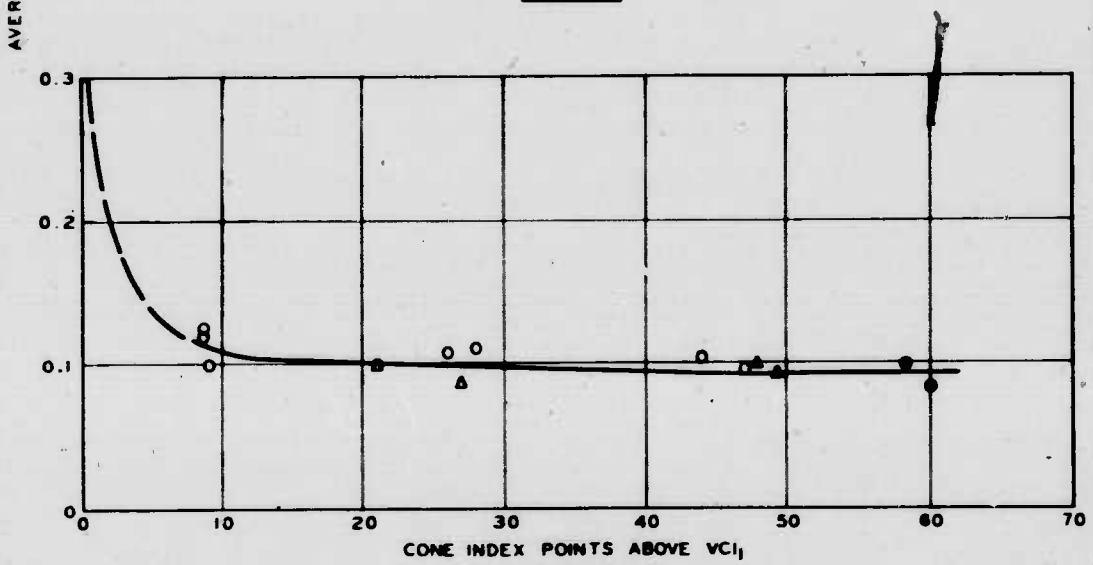

c. SUMMARY

LEGEND

OPEN SYMBOLS INDICATE BARE SURFACES
CLOSED SYMBOLS INDICATE GRASS-COVERED SURFACES.
NUMBERS NEAR PLOTTED POINTS ARE CODE NUMBERS FROM TABLES F2 AND F4.

DECELERATION RELATIONS FOR TRACKED VEHICLES

PLATE F4

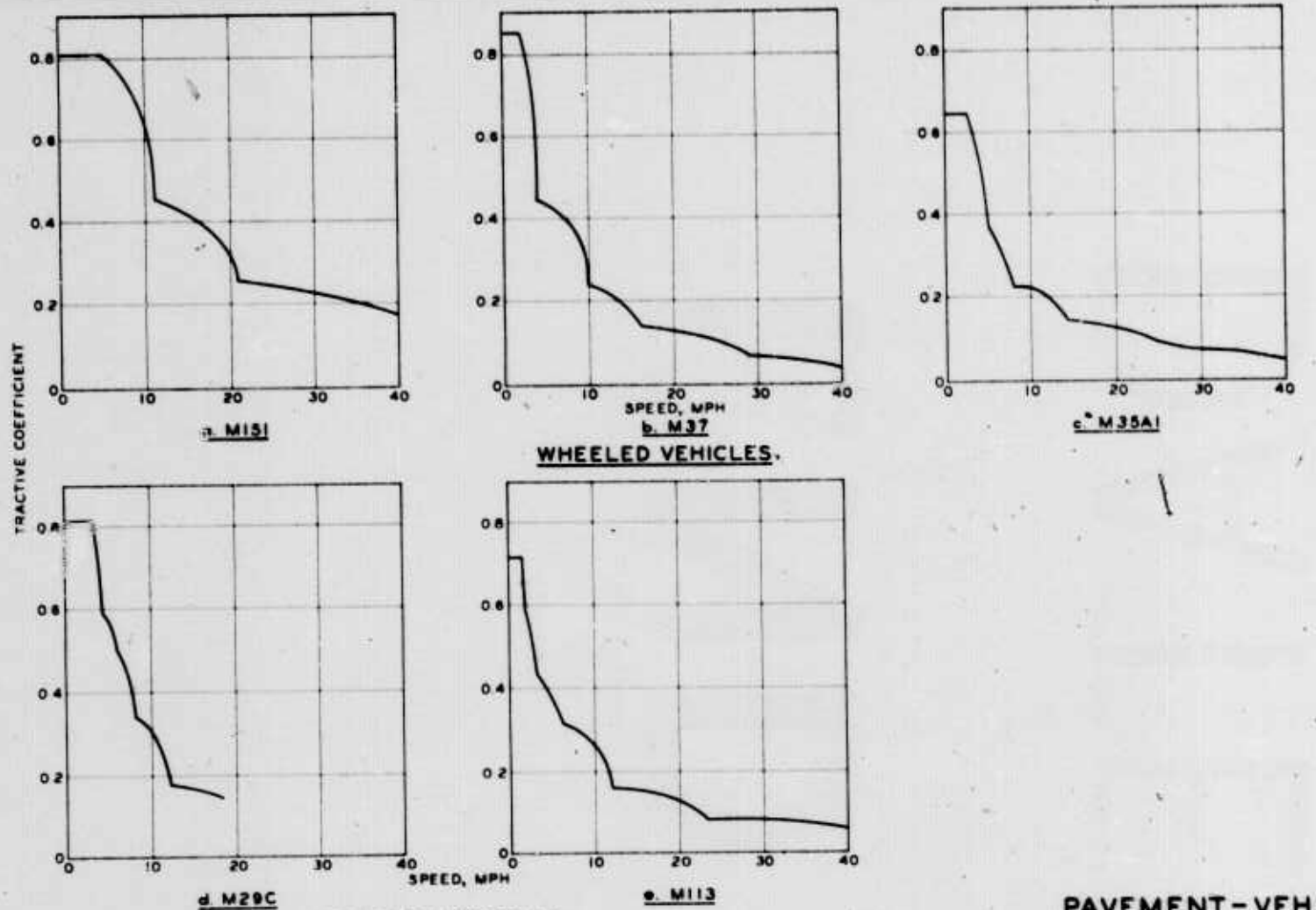

PAVEMENT-VEHICLE RELATIONS

PAGE 35

PLATE F9

THE COMPUTATIONS MADE TO ACCOUNT FOR THE EFFECTS OF THE GEAR CHANGE INDICATED BY SINGLE ASTERISKS (*) IN TABLE F8 AND PLATE F8 ARE EXPLAINED BELOW.

THE SPEED AT WHICH THE GEAR CHANGE SHOULD OCCUR WAS DETERMINED FROM THE DRAWBAR PULL COEFFICIENT (DBP/W)-SPEED CURVE (FIG. 1).

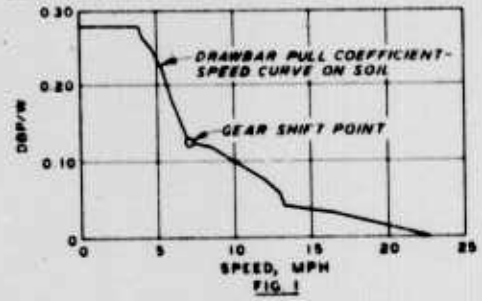

FIG. 1

THE PREDICTION SCHEME PRESUMES THAT WHEN THE VEHICLE HAS ACCELERATED TO THE SPEED INDICATED ON DBP COEFFICIENT-SPEED CURVE (FIG. 1), THE GEAR CHANGE WILL COMMENCE AND THAT THE VEHICLE WILL DECELERATE FOR AN ARBITRARY TIME INCREMENT OF 0.4 SEC, THEN ACCELERATE TO THE SPEED AT WHICH THE GEAR CHANGE BEGAN (FIG. 2).

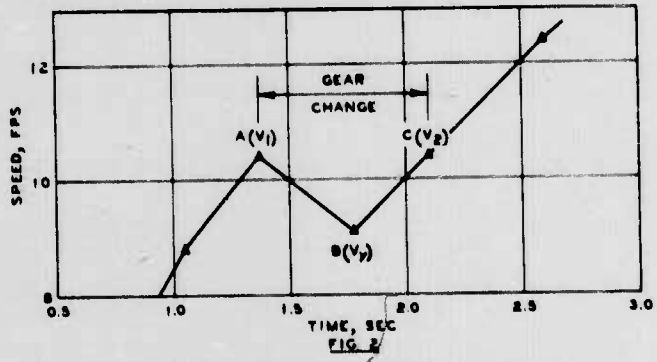

FIG. 2

IN FIG. 2 POINT A REPRESENTS THE SPEED (10.41 FPS)* AT WHICH THE GEAR CHANGE BEGINS. THE VEHICLE DECELERATES FOR 0.4 SEC. THE SPEED AT POINT B IS DETERMINED BY THE EQUATION

$$\frac{V_1 - V_y}{t} = -a \qquad (1)$$

* VALUES USED AND DEVELOPED ARE GIVEN IN TABLE F8.

IN EQUATION 1, V_1 IS KNOWN (FROM THE DRAWBAR-SPEED CURVE), t IS AN ARBITRARY 0.4 SEC, AND $-a$ IS KNOWN (PARAGRAPH 36). THE EQUATION IS SOLVED FOR V_y IN THE FOLLOWING MANNER

$$\frac{10.41 - V_y}{0.4} = -(0.100)(32.16)$$

$$V_y = 9.12 \text{ FPS} = 6.22 \text{ MPH}$$

IN FIG. 2 THE VEHICLE THEN ACCELERATES FROM POINT B TO POINT C, I.E., FROM THE SPEED V_y AT THE END OF THE INCREMENT OF DECELERATION TO THE SPEED V_2 AT WHICH THE GEAR CHANGE BEGAN. THE TIME t REQUIRED TO ACCELERATE FROM V_y TO V_2 IS DETERMINED BY THE FOLLOWING EQUATION

$$\frac{V_2 - V_y}{t} = a \qquad (2)$$

IN EQUATION 2, V_y IS KNOWN ($V_y = V_1$ = SPEED AT WHICH GEAR CHANGE BEGAN), a IS KNOWN $\left(\frac{DBP}{W} \cdot g\right.$, PARAGRAPH 36; HOWEVER, $\frac{DBP}{W}$ IS LIMITED TO THE MAXIMUM $\frac{DBP}{W}$ THAT CAN BE DEVELOPED IN THE HIGHER GEAR$\left.\right)$. THE EQUATION IS SOLVED FOR t IN THE FOLLOWING MANNER

$$\frac{10.41 - 9.12}{t} = (0.129)(32.16)$$

$$t = 0.32 \text{ SEC}$$

FOR THE INCREMENT OF ACCELERATION AND FOR THE INCREMENT OF DECELERATION, THE DISTANCE TRAVELED IS DETERMINED BY MULTIPLYING THE AVERAGE VELOCITY BY THE TIME AS FOLLOWS.

FOR INCREMENT OF DECELERATION

$$\bar{V}(t) = d$$

$$\frac{10.41 + 9.12}{2}(0.4) = d$$

$$d = 3.91 \text{ FT}$$

FOR INCREMENT OF ACCELERATION

$$\bar{V}(t) = d$$

$$\frac{9.12 + 10.41}{2}(0.32) = d$$

$$d = 3.12 \text{ FT}$$

COMPUTATIONS OF THE EFFECTS OF A GEAR CHANGE WHILE ACCELERATING

THE COMPUTATIONS MADE TO PREDICT THE SPEED, DISTANCE, AND TIME AT THE POINT OF INTERSECTION OF THE ACCELERATION AND DECELERATION CURVES (PLATE F8) AND THE DETERMINATION OF THE AVERAGE PREDICTED SPEED FOR TEST 269R USING THE WES CURVES ARE OUTLINED BELOW.

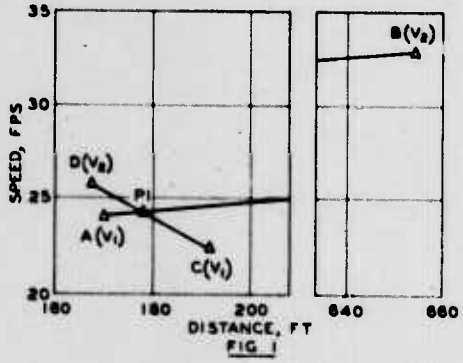

FIG. 1

LINE	SPEED AT START OF INCREMENT V_1, FPS	SPEED AT END OF INCREMENT V_2, FPS	DISTANCE AT START OF INCREMENT d_1, FT	DISTANCE AT END OF INCREMENT d_2, FT
AB	24.18	32.84	170.17	654.27
CD	32.51	25.73	191.51	167.99

▲ PI = POINT OF INTERSECTION

THE LINE AB IN FIG. 1 REPRESENTS THE INCREMENT OF THE ACCELERATION CURVE WHEREIN THE INTERSECTION WITH THE DECELERATION CURVE OCCURS (SEE PLATE F8). THE LINE CD IN FIG. 1 REPRESENTS THE INCREMENT OF THE DECELERATION CURVE WHEREIN THE INTERSECTION WITH THE ACCELERATION CURVE OCCURS. THE POINT OF INTERSECTION IS DETERMINED BY THE SIMULTANEOUS SOLUTION OF THE EQUATIONS OF THE TWO LINES.

THE EQUATIONS OF THE LINES AB AND CD ARE DEVELOPED FROM THE GENERAL EQUATION

$$v_y = \frac{v_2 - v_1}{d_2 - d_1}(d_y) + C \qquad (1)$$

FOR LINE AB

$$\frac{v_2 - v_1}{d_2 - d_1} = \frac{32.84 - 24.18}{654.27 - 170.17} = 0.0178$$

LET $v_y = v_1$, $d_y = d_1$

$$24.18 = 0.0178(170.17) + C$$
$$C = 21.15$$

THE EQUATION OF LINE AB IS THEN

$$v_y = 0.0178d_y + 21.15 \qquad (2)$$

FOR ANY DISTANCE BETWEEN d_1 AND d_2

FOR LINE CD

$$\frac{v_2 - v_1}{d_2 - d_1} = \frac{25.73 - 32.51}{167.99 - 191.51} = 0.1334$$

LET $v_y = v_1$, $d_y = d_1$

$$32.51 = 0.1334(191.51) + C$$
$$C = 48.06$$

THE EQUATION FOR LINE CD IS THEN

$$v_y = 48.06 - 0.1334d_y \qquad (3)$$

FOR ANY DISTANCE BETWEEN d_1 AND d_2

THE DISTANCE d_y AT THE POINT OF INTERSECTION IS FOUND BY SETTING EQUATION 2 EQUAL TO EQUATION 3.

$$0.0178d_y + 21.15 = 48.06 - 0.1334d_y$$
$$d_y = 177.98 \text{ FT}$$

THE SPEED AT THE POINT OF INTERSECTION IS FOUND BY SUBSTITUTING THE DISTANCE (177.98 FT) INTO EQUATION 2 OR EQUATION 3.

EQUATION 2

$$V_y = 0.0178(177.98) + 21.15$$
$$V_y = 24.32 \text{ FPS} = 16.58 \text{ MPH}$$

EQUATION 3

$$V_y = 48.06 - 0.1334(177.98)$$
$$V_y = 24.32 \text{ FPS} = 16.58 \text{ MPH}$$

THE TIME REQUIRED FOR THE INCREMENT OF ACCELERATION FROM A TO C (FIG. 1) AND THE TIME REQUIRED FOR DECELERATION FROM C TO C IS FOUND BY USING THE GENERAL EQUATION

$$d_t = Vt_s$$

WHERE

d_t = DISTANCE, FT
V = AVERAGE SPEED, FPS
t = TIME, SEC

FOR LINE A PI

$$d_y - d_1 = \frac{V_1 + V_y}{2} t_s \qquad (5)$$

$$177.98 - 170.17 = \frac{24.18 + 24.32}{2} t_s$$

$$t_s = 0.32 \text{ SEC}$$

THE TOTAL TIME FOR ACCELERATION IS FOUND BY ADDING 0.32 SEC TO THE CUMULATIVE TIME AT POINT A (10.26 SEC, FROM TABLE F8).

THUS

TOTAL TIME TO ACCELERATE IS

$10.26 + 0.32 = 10.58$ SEC

FOR LINE C PI

$$d_1 = d_y - \frac{V_1 + V_y}{2} t_s \qquad (6)$$

$$191.51 = 177.98 - \frac{32.51 + 24.32}{2} t_s$$

$$t_s = 0.58 \text{ SEC}$$

THE TOTAL TIME FOR DECELERATION IS FOUND BY ADDING 0.5 SEC TO THE TIME AT POINT C (7.7 SEC, FROM TABLE F8).

THUS

TOTAL TIME TO DECELERATE IS

$7.7 + 0.58 = 7.58$ SEC

FINALLY, THE TOTAL DISTANCE, 220.3 FT, IS DIVIDED BY THE SUM OF THE TIME REQUIRED TO ACCELERATE AND THE TIME REQUIRED TO DECELERATE.

PREDICTED AVERAGE SPEED $\frac{220.3}{18.16} = 14.48 \text{ FPS} = 10.1 \text{ MPH}$

COMPUTATIONS MADE TO DETERMINE PREDICTED AVERAGE SPEED

M35A1, TEST 269R

PLATE F9

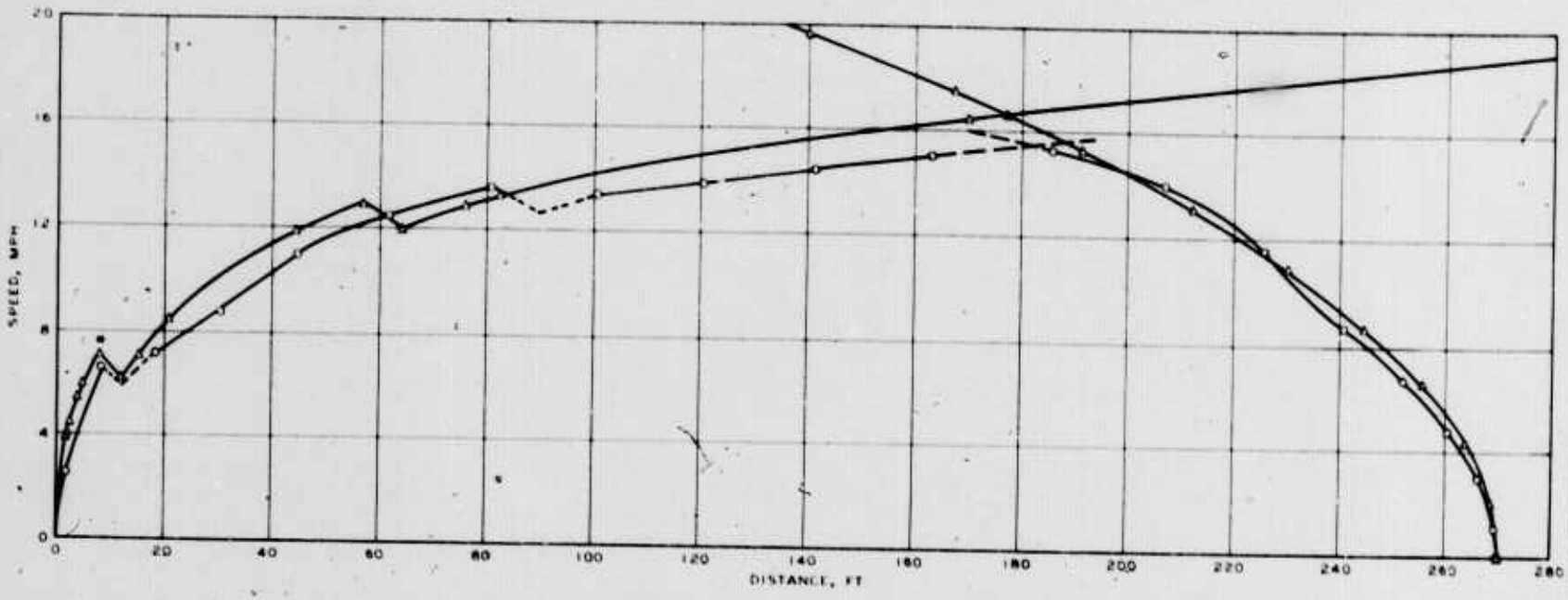

LEGEND

- ○ MEASURED, TABLE F10 (SPEED AT MIDPOINT OF DISTANCE INCREMENT)
- △ PREDICTED USING WES CURVES, TABLES F8 AND F9
- ▲ POINT OF INTERSECTION OF PREDICTED CURVES, PLATE F7
- ----- INCREMENTS WHEREIN GEAR SHIFTS OCCURRED
- * FOR EXPLANATION OF COMPUTATIONS OF THE EFFECTS OF GEAR CHANGES ON THE PREDICTED ACCELERATION CURVES, SEE PLATE F8.

COMPARISON OF MEASURED AND PREDICTED PERFORMANCES

M35A1, SITE 4V-S-3, TEST 269 R

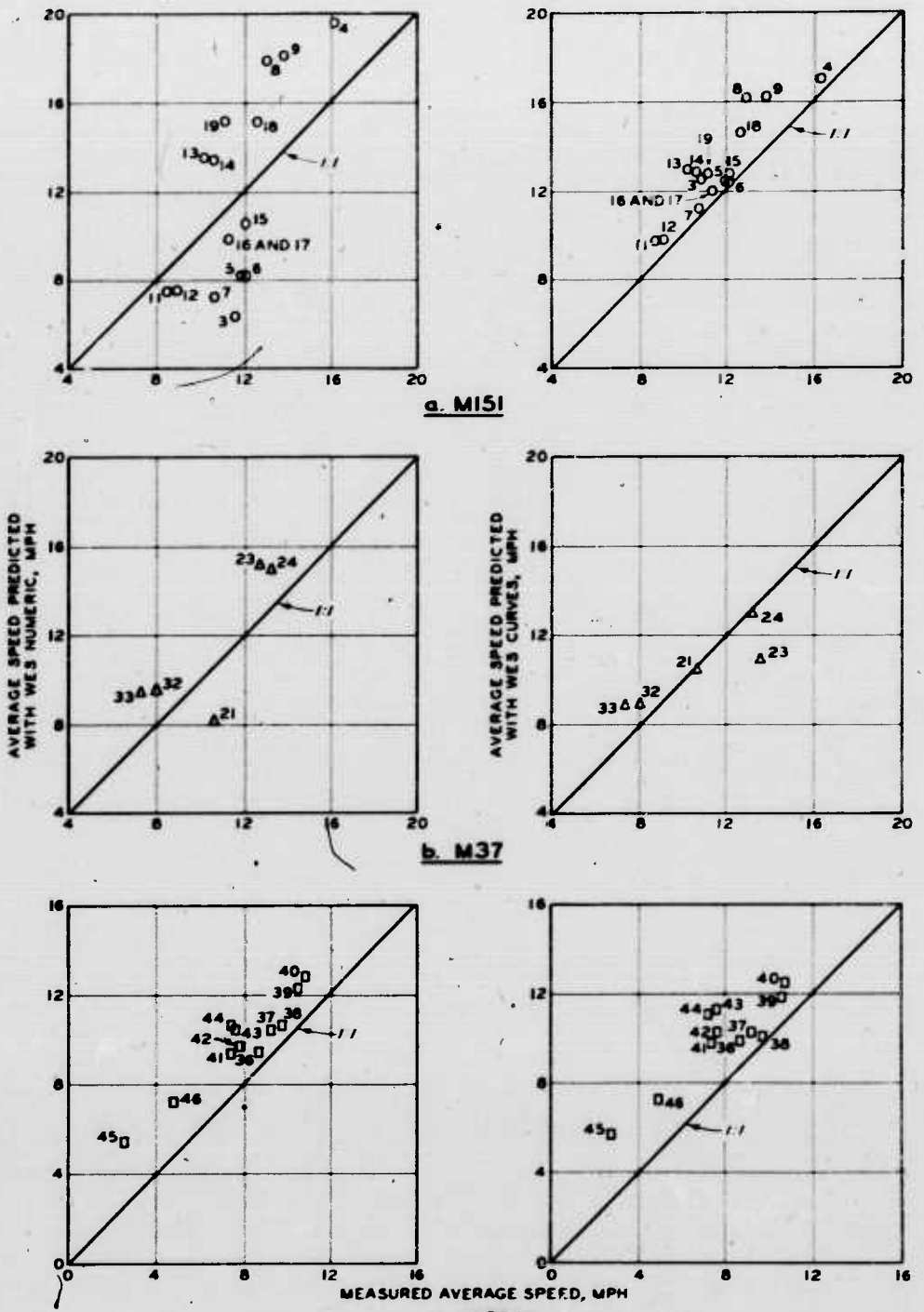

NOTE: SMALL NUMBERS NEAR PLOTTED POINTS ARE CODE NUMBERS FROM TABLE F2.

COMPARISON OF PREDICTED AND MEASURED AVERAGE SPEEDS FOR WHEELED VEHICLES

PLATE F9

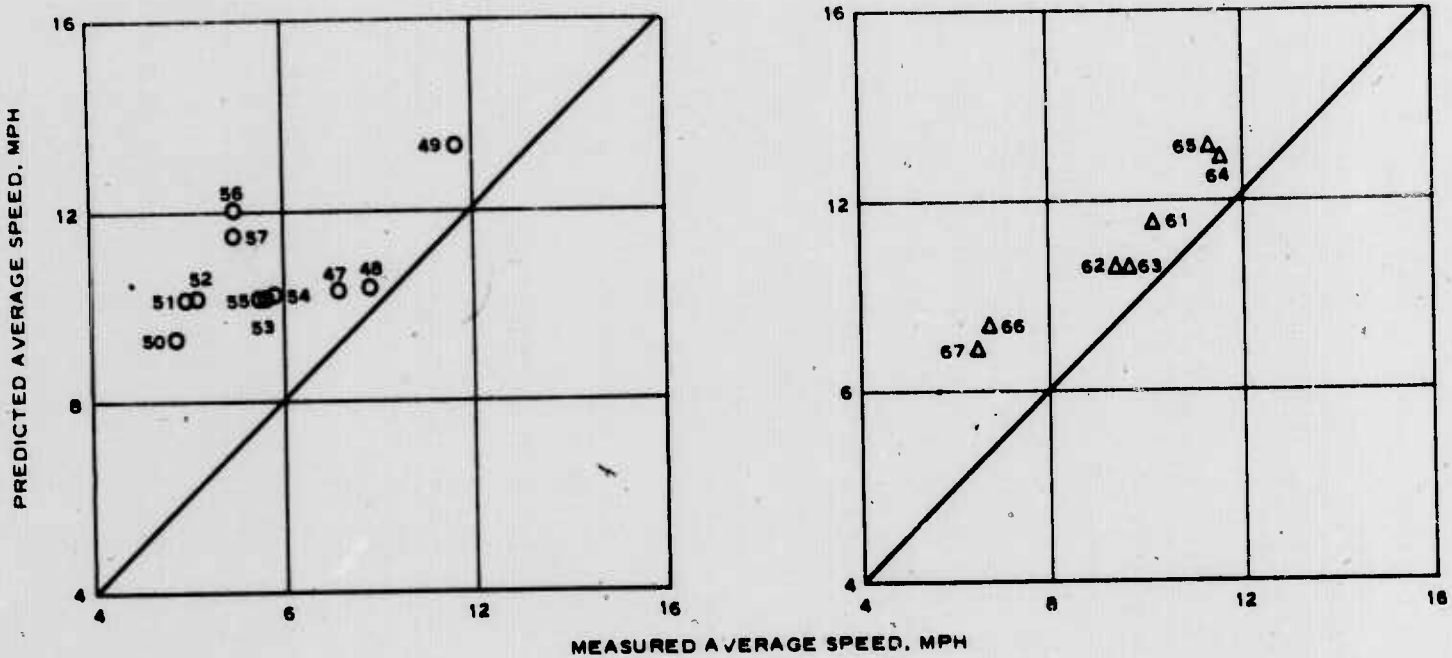

a. M29C

b. M113

NOTE: NUMBERS NEAR PLOTTED POINTS ARE CODE NUMBERS FROM TABLE F2.

COMPARISON OF PREDICTED AND MEASURED AVERAGE SPEEDS FOR TRACKED VEHICLES

DISTRIBUTION LIST FOR TR 3-783, APPENDIX F

Address*	No. of Copies
Army	
Chief of Engineers, Department of the Army, Washington, D. C. 20314	
ATTN: ENGSA	2
ENGME	1
ENGME-M	2
ENGME-S	1
Chief of Research and Development, Headquarters Department of the Army, Washington, D. C. 20310 ATTN: Director of Army Technical Information	3 copies of Form 1473
Assistant Chief of Staff for Force Development, Department of the Army, Washington, D. C. 20315 ATTN: FOR DS SSS, The Pentagon	1
Secretary of Defense, Washington, D. C. 20315 ATTN: ARPA/AGILE, The Pentagon	4
Commanding Officer, Defense Intelligence Agency, Washington, D. C. 20301 ATTN: DIAAP-1E	1
Commanding General, U. S. Army Materiel Command, Washington, D. C. 20315 ATTN: AMCRD-RV-E	2
Commanding General, U. S. Army Tank-Automotive Center, Warren, Mich. 48090 ATTN: AMSTA-BSL	2
Commanding General, U. S. Army Natick Laboratories, Natick, Mass. 01760 ATTN: AMXRE-ED (Dr. L. W. Trueblood)	2
Commanding General, U. S. Army Topographic Command, Washington, D. C. 20315	1
Commanding General, U. S. Army Forces Southern Command, Fort Amador, Canal Zone ATTN: Engineer	1
Commanding General, U. S. Army Electronic Proving Ground, Fort Huachuca, Ariz. 85613 ATTN: Library	1
Commanding General, U. S. Continental Army Command, Fort Monroe, Va. 23351 ATTN: Combat Development (ATSND)	1
Commanding General, U. S. Continental Army Command Engineering Division, DCSLOG, Fort Monroe, Va. 23351 ATTN: ATLOG-E-MB	1
Commanding General, U. S. Army Weapons Command, Rock Island, Ill. 61201 ATTN: AMSWE-RDR	1
Commanding Officer, Special Warfare Agency Fort Bragg, N. C. 28307	1
Commanding Officer, U. S. Army Limited War Laboratory, Aberdeen Proving Ground, Md. 21005 ATTN: Development Engineering Division	1
Director, OSD/ARPA R&D Field Unit, APO San Francisco 96346	35
Director, OSD/ARPA Regional Field Office, ARMISH-MAAG (RFO-I), APO New York 09205	1
Director, OSD/ARPA R&D Field Unit, APO San Francisco 96243	2

* Addressees: please notify U. S. Army Engineer Waterways Experiment Station, Vicksburg, Miss. 39180, of any change in address.

Address	No. of Copies
Army (Continued)	
Commanding Officer, U. S. Army Combat Developments Command Experimentation Center Fort Ord, Calif. 93941	1
Commanding Officer, U. S. Army Rock Island Arsenal, Rock Island, Ill. 61201	1
Commanding Officer, U. S. Army Aviation Materiel Laboratory, Fort Eustis, Va. 23604 ATTN: OSMFE-ES (Mr. H. P. Simon)	1
Commanding Officer, U. S. Army Mobility Equipment Research and Development Center Fort Belvoir, Va. 22060 ATTN: Technical Documents Center, Bldg 315	1
Commander, U. S. Military Assistance Command, APO San Francisco 96346	2
Commander, U. S. Army Combat Development Command Engineer Agency, Fort Belvoir, Va. 22060 ATTN: CSGEN-M	1
Commander, Picatinny Arsenal, Engineer Research Section, Dover, N. J. 07801 ATTN: Ammunition Research Laboratory	1
Commandant, U. S. Army Engineer School, Fort Belvoir, Va. 22060 ATTN: Library	1
Commandant, Armed Forces Staff College, Norfolk, Va. 23511 ATTN: Library	1
Commandant, U. S. Army Signal School, Fort Monmouth, N. J. 07703 ATTN: Library	1
Commandant, U. S. Military Academy, West Point, N. Y. 10996 ATTN: Library	1
Commandant, Command and General Staff College, Fort Leavenworth, Kans. 66027 ATTN: Archives	1
Director, U. S. Army Development and Proof Services, Aberdeen Proving Ground, Md. 21005 ATTN: Technical Library Automotive Engineering Laboratory (STEAP-DS-LU) Automotive Division (STEAP-DS-TU)	2 1 1
Director, Institute for Defense Analysis, 400 Army-Navy Drive, Arlington, Va. 22202	1
President, U. S. Army Artillery Board, Fort Sill, Okla. 73503	1
President, U. S. Army Aviation Test Board, Fort Rucker, Ala. 36360	1
President, U. S. Army Air Defense Board, Fort Bliss, Tex. 79916	1
President, U. S. Army Infantry Board, Fort Benning, Ga. 31905 ATTN: Tactical Section, TIS	1
President, U. S. Army Infantry Board, Fort Benning, Ga. 31905	1
President, U. S. Army Armor Board, Fort Knox, Ky. 40121	1
CINCPAC, Camp H. M. Smith, Oahu, Hawaii 96822	2
LTC E. W. Stewart, U. S. Army Combat Developments Command, Institute of Land Combat Fort Belvoir, Va. 22060	1
President, U. S. Army Airborne, Electronic-Special Warfare Board, Fort Bragg, N. C. 28307	1
Director, U. S. Army Cold Regions Research and Engineering Laboratory, P. O. Box 282, Hanover, N. H. 03755 ATTN: AMXCR-PI (Mr. R. E. Frost) Library	2 1

Address	No. of Copies
Navy	
Commanding Officer, Office of Naval Research, Surface and Amphibious Programs (Code 463) Washington, D. C. 20390 ATTN: Naval Applications Group	1
Commanding Officer, PHIBCB One, U. S. Naval Amphibious Base, Coronado, San Diego, Calif. 92118	1
Commanding Officer, PHIBCB Two, U. S. Naval Amphibious Base, Little Creek, Norfolk, Va. 23521	1
Commanding Officer, Office of Naval Research, Washington, D. C. 20390 ATTN: Earth Sciences Division (Code 410)	1
Commanding Officer, U. S. Naval Photographic Interpretation Center, 4301 Suitland Road, Washington, D. C. 20390 ATTN: Library	1
Commanding Officer and Director, U. S. Naval Civil Engineering Lab, Port Hueneme, Calif. 93041	1
Commandant, U. S. Marine Corps, Washington, D. C. 20380 ATTN: AO4E	1
Chief, Naval Facilities Engineering Command, Washington, D. C. 20360 ATTN: Code 70, Department of the Navy	1
Director, Naval Warfare Research Center, Stanford Research Institute, Menlo Park, Calif. 94025	1
U. S. Army Attache, American Embassy, U. S. Navy, Box 36, FPO New York 09510	2
Air Force	
Headquarters, USAF, Washington, D. C. 20330	
ATTN: Deputy Chief of Staff, Research and Development (AFRDC)	1
Deputy Chief of Staff, Director of Civil Engineering (AFOCE)	1
Director of Science and Technology (AFRST)	1
Air Force Office of Scientific Research, Building T-D, Washington, D. C. 20330	1
Commander, Air Proving Ground Center, Eglin AFB, Fla. 32542 ATTN: ADTC (ADBPS-12)	1
Commander, U. S. Strike Command, MacDill AFB, Fla. 33608 ATTN: J4-E	1
Director, Terrestrial Sciences Laboratory (CRJT), Air Force, Cambridge Research Laboratories, L. G. Hanscom Field, Bedford, Mass. 01730	1
Air University Library, Maxwell AFB, Ala. 36112	1

Address	No. of Copies
Other Government Agencies	
Defense Documentation Center, Cameron Station, Alexandria, Va. 22314 ATTN Mr. Myer Kahn	20
Library, Division of Public Documents (NO CLASSIFIED REPORTS TO THIS ADDRESS), U. S. Government Printing Office, Washington, D. C. 20402	1
Library of Congress, Documents Expediting Project, Washington, D. C. 20540	3
Director, Project Michigan, Willow Run Laboratories, Ypsilanti, Mich. 48197	1
Chief, Source Material Unit, Branch of Military Geology, U. S. Geological Survey Washington, D. C. 20242	2
Chief, World Soil Geography Unit, Soil Survey Interpretations, USDA Soil Conservation Service 14th St. and Independence Ave. SW, Washington, D. C. 20250	2
National Tillage Machinery Laboratory, U. S. Dept. of Agriculture, P. O. Box 792 Auburn, Ala. 36830	1
Colleges and Universities	
University of Arkansas, College of Engineering, Fayetteville, Ark. 72701	1
Dr. Daniel C. Drucker, Dean, College of Engineering, University of Illinois, Urbana, Ill. 61801	1
Massachusetts Institute of Technology, Cambridge, Mass. 02139 ATTN Soil Engineering Library	1
Dr. Emil H. Jebe, Operations Research Dept., Institute of Science and Technology, University of Michigan, Box 618, Ann Arbor, Mich. 48106	1
Prof. L. C. Stuart, University of Michigan, Ann Arbor, Mich. 48104	1
Prof. Ralph E. Fadum, Dean, School of Engineering, North Carolina State College of the University of North Carolina, Raleigh, N. C. 27607	1
Davidson Laboratory, Stevens Institute of Technology, 711 Hudson Street, Hoboken, N. J. 07030	1
New York University, University Heights, Bronx, N. Y. 10453 ATTN Engineering Library	1
Other	
Battelle Memorial Institute, 1755 Massachusetts Avenue, N. W., Washington, D. C. ATTN RACIC	1
Engineering Societies Library, 345 E. 47th Street, New York, N. Y. 10017	1
GM Defense Research Laboratories, General Motors Corporation, Box T, Santa Barbara, Calif. 93101	1
Prof. Robert Horonjeff, 3643 Brook Street, Lafayette, Calif. 94549	1
Research Analysis Corporation, McLean, Va. 22101 ATTN Library	1
WNRE, Inc., Chestertown, Md. 21620 ATTN Mr. C. J. Nuttall, Jr.	2

Unclassified

Security Classification

DOCUMENT CONTROL DATA - R & D

(Security classification of title, body of abstract and indexing annotation must be entered when the overall report is classified)

1. ORIGINATING ACTIVITY (Corporate author)
U. S. Army Engineer Waterways Experiment Station
Vicksburg, Miss.

2a. REPORT SECURITY CLASSIFICATION
Unclassified

2b. GROUP

3. REPORT TITLE
AN ANALYTICAL MODEL FOR PREDICTING CROSS-COUNTRY VEHICLE PERFORMANCE:
APPENDIX F: SOIL-VEHICLE RELATIONS ON SOFT CLAY SOILS (SURFACE COMPOSITION)

4. DESCRIPTIVE NOTES (Type of report and inclusive dates)
Appendix F to final report

5. AUTHOR(S) (First name, middle initial, last name)
Claude A. Blackmon

6. REPORT DATE	7a. TOTAL NO. OF PAGES	7b. NO. OF REFS
August 1970	62	8

8a. CONTRACT OR GRANT NO.	9a. ORIGINATOR'S REPORT NUMBER(S)
ARPA Order No. 400	Technical Report No. 3-783, Appendix F
b. PROJECT NO. 1-T-0-62112-A-131 and 1-T-0-62103-A-046-02	
c.	9b. OTHER REPORT NO(S) (Any other numbers that may be assigned this report)
d.	

10. DISTRIBUTION STATEMENT
This document is subject to special export controls and each transmittal to foreign governments or foreign nationals may be made only with prior approval of U. S. Army Engineer Waterways Experiment Station.

11. SUPPLEMENTARY NOTES	12. SPONSORING MILITARY ACTIVITY
	Advanced Research Projects Agency and Directorate of Development and Engineering, U. S. Army Materiel Command

13. ABSTRACT

Sixty-six acceleration-deceleration tests were conducted with three wheeled and two tracked vehicles at five sites in Thailand. The principal conclusion from these tests was that vehicle deceleration in soft clay soils can be correlated with soil strength expressed as the average 0- to 6-in. cone index. The analysis indicated that acceleration increased with an increase in soil strength, but no definitive correlation could be established. Semiempirical and empirical relations were used in a first-generation analytical model to predict average speed over the test courses. Comparisons of measured and predicted speeds led to recommendations for specific additional studies to improve the reliability of the WES analytical model.

DD FORM 1 NOV 68 1473 REPLACES DD FORM 1473, 1 JAN 64, WHICH IS OBSOLETE FOR ARMY USE.

Unclassified

Security Classification

14 KEY WORDS	LINK A		LINK B		LINK C	
	ROLE	WT	ROLE	WT	ROLE	WT
Clays						
Cross-country tests						
Mathematical models						
Military vehicles						
Soft soils						
Soil-vehicle interaction						
Thailand						
Trafficability						